UNIVERSITATEA DIN BUCUREȘTI
VIRTUTE ET SAPIENTIA

Satellite Mega-constellations: operational risks and the impact on ground-based astronomical observations

PhD Candidate
Cristian OMĂT

PhD Supervisor
Professor Mirel BÎRLAN

Presentation Structure

Scope of the Thesis

- ❑ the study of artificial near-Earth objects in the context of satellite constellations
- ❑ the impact on ground-based astronomical observations

Chapter 1: The Mega-Constellation Paradigm

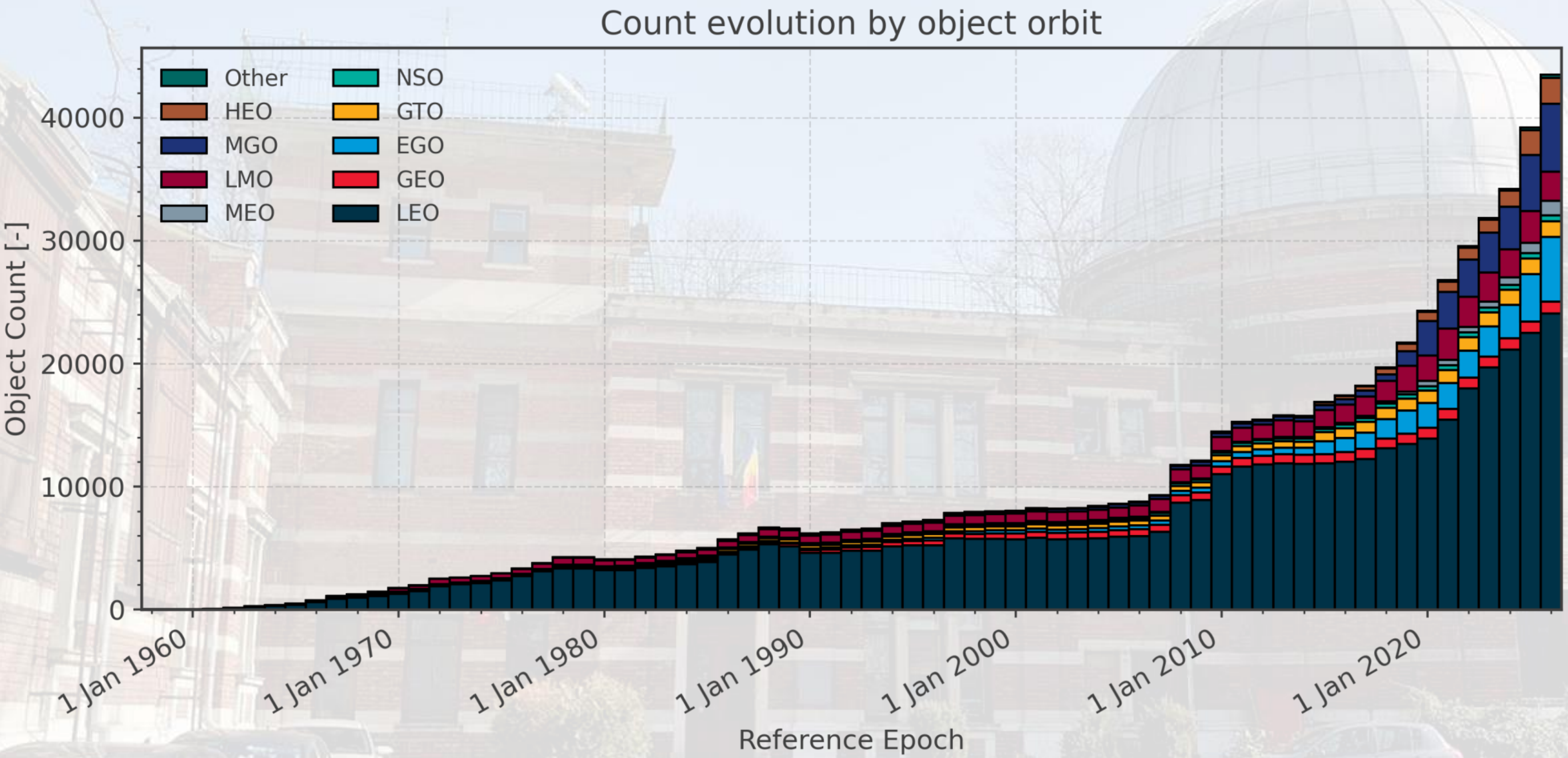

Credit: ESA (Annual Report 2025)

Forecast: approximately 100,000 satellites will be deployed into LEO orbits by the end of 2030 (Boley and Byers, 2021)

11 : total number of constellations

11,582 : total number of launched satellites

9,201 : total number of operational satellites

1,896,629 : total number of satellites for which deployment licenses into LEO orbits have been requested

➔ 246% annual growth

Credit: Jonathan McDowell, https://planet4589.org, (March 2026)

Orbital Density of the Starlink Mega-Constellation

EQ view

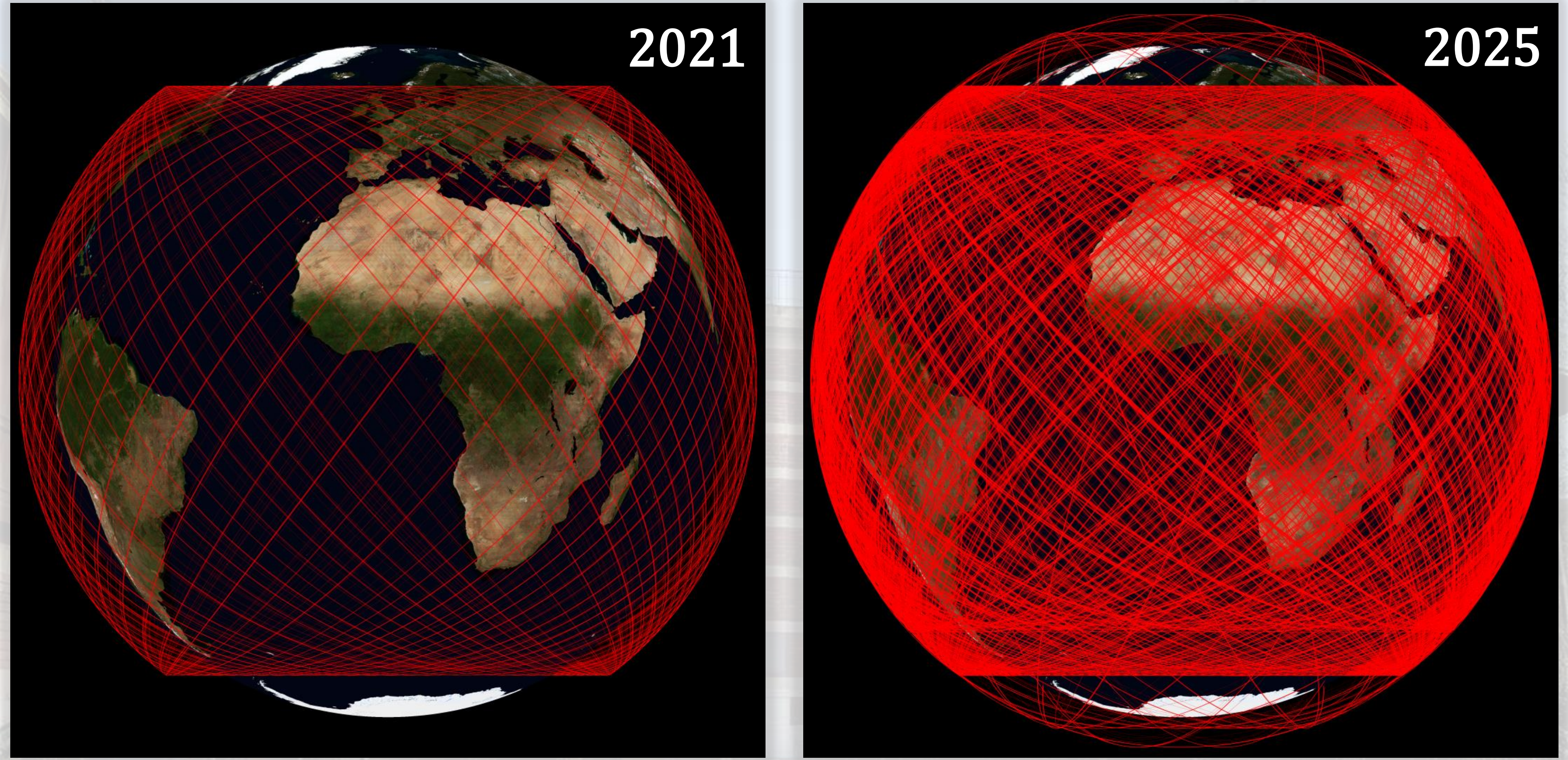

Simulation: Astronomical Institute of the Romanian Academy (AIRA)

Orbital Density of the Starlink Mega-Constellation

Polar view

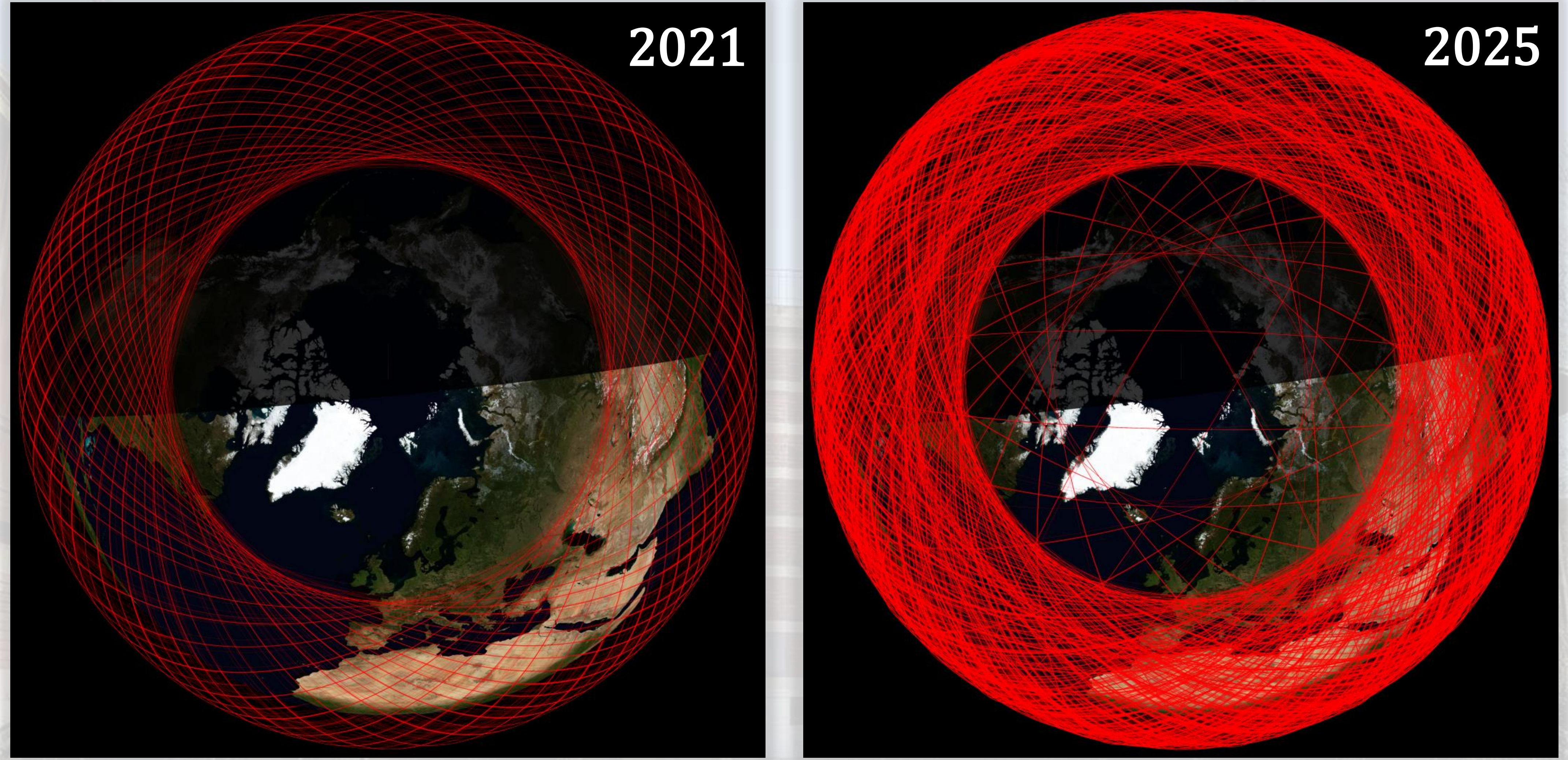

Simulation: Astronomical Institute of the Romanian Academy (AIRA)

Kessler Syndrome

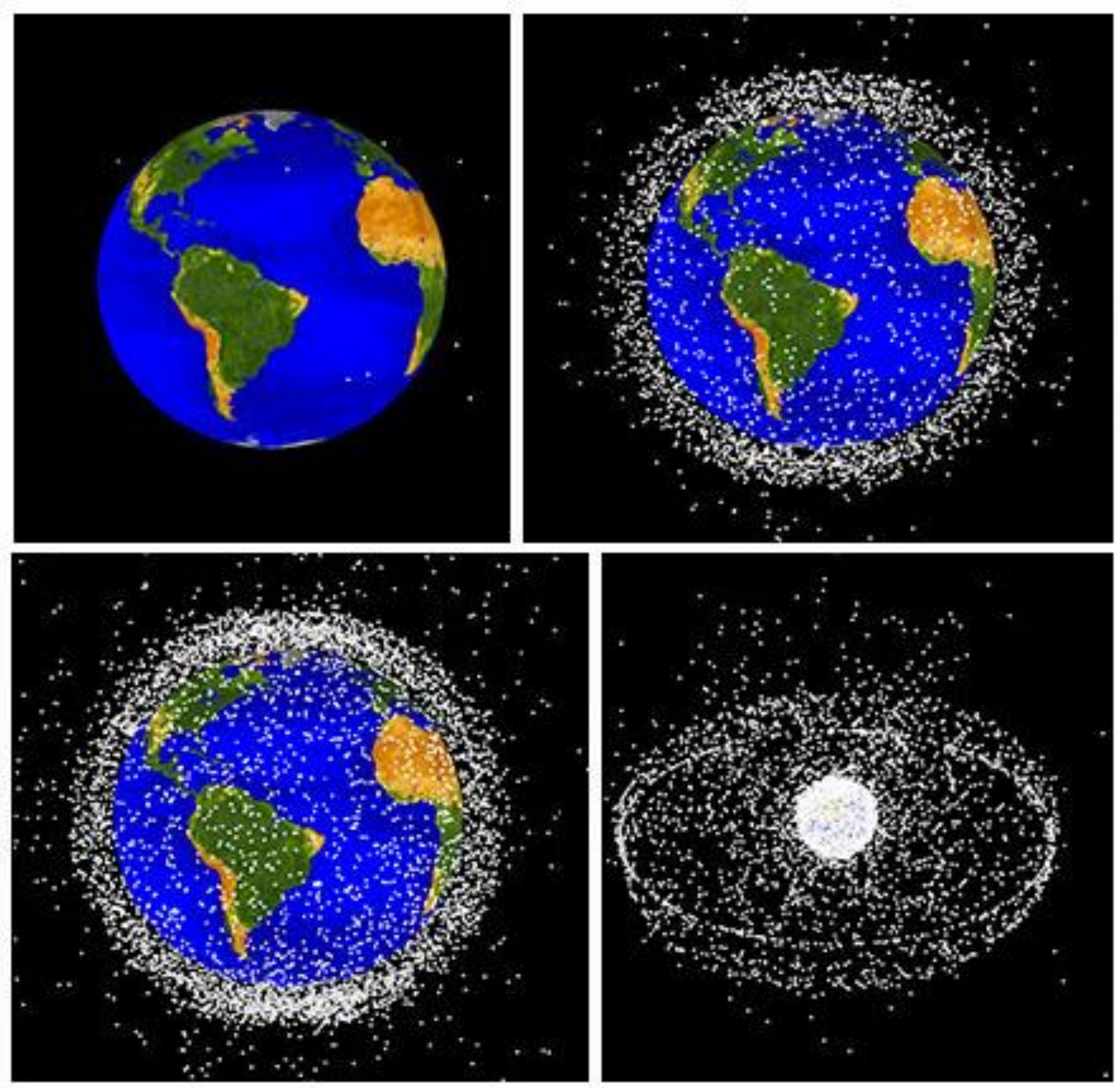

Credit: *ESA*

- the saturation of Low Earth Orbits (LEO) with satellites and space debris
- the exponential increase in the number of collisions between objects
- a self-sustaining collisional cascade, capable of isolating Earth for extended periods of time

(Kessler and Cour-Palais, 1978)

Key Technological Enablers

Miniaturization, the adoption of COTS components, and Reusable Launch Vehicles (RLVs) have led to:

- reduction in satellite size, mass, and power consumption (SWaP)
- faster access to advanced commercial technologies
- increased economic feasibility of satellite constellations

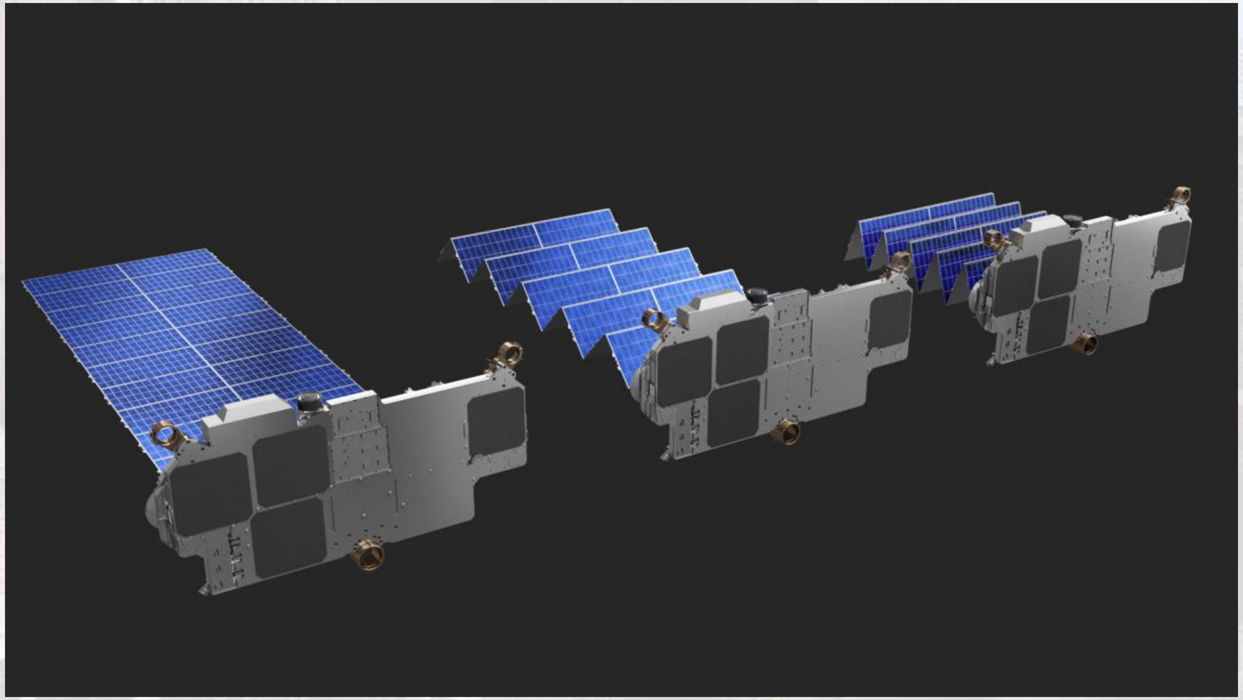

Credit: www.cgtrader.com / www.gdca.com

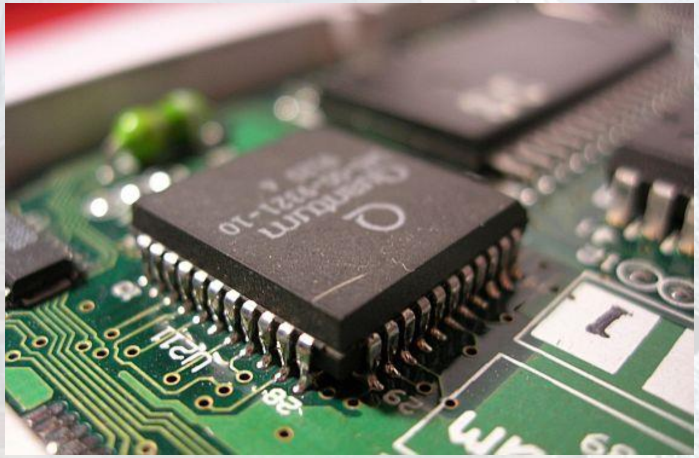

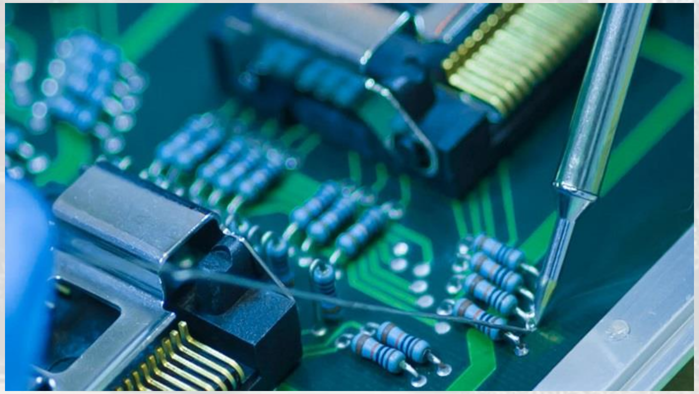

Chapter 2: Operational Risks in Low Earth Orbit (LEO)

Operational Risk	Main Effect
Collision and Fragmentation	collisions, fragmentations, and the increasing density of orbital debris
Radiation Environment	degradation of electronic components and the onset of functional anomalies
Electromagnetic Interference (EMI)	disruption of satellite communications, navigation, and control
Orbital Decay and Attitude Control Degradation	reduction in orbital altitude and compromised mission stability

Chapter 3: Applied Orbital Mechanics in LEO

ECI – Earth Centered Inertial

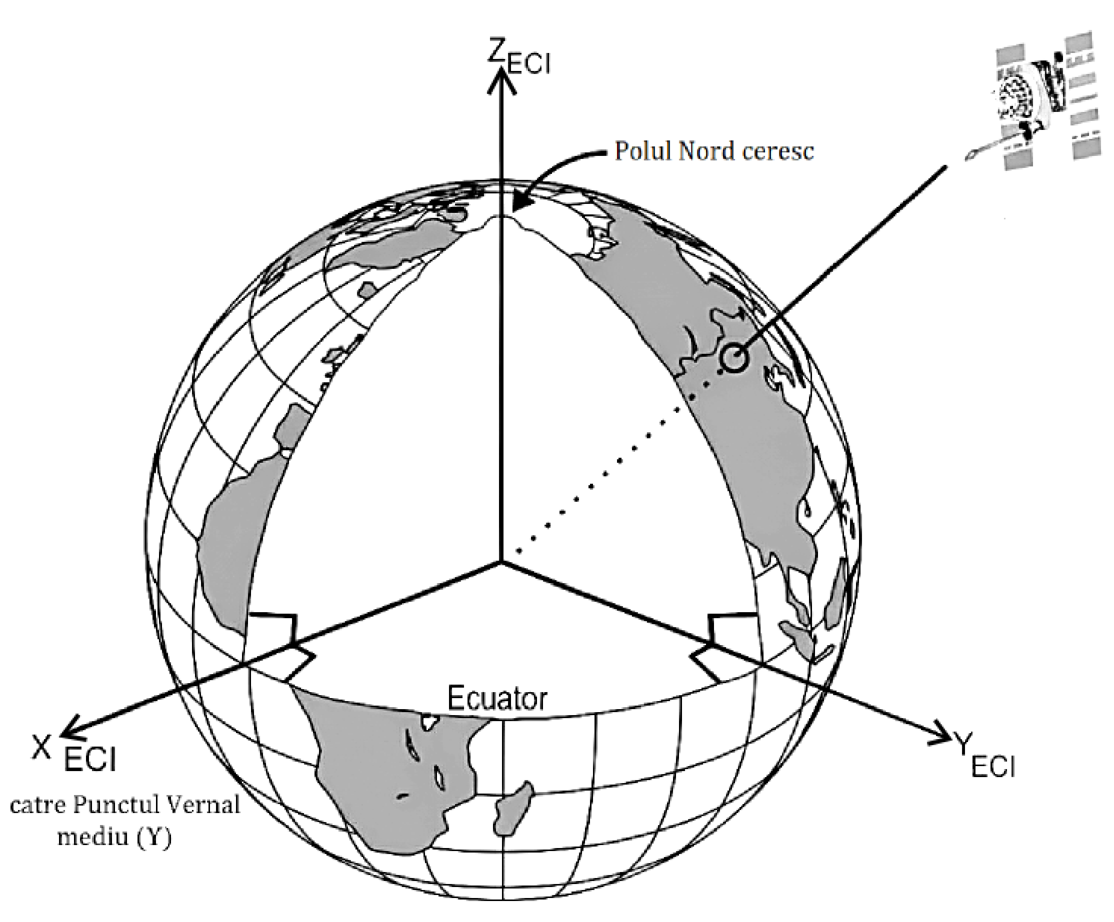

ECEF - Earth-Centered Earth-Fixed

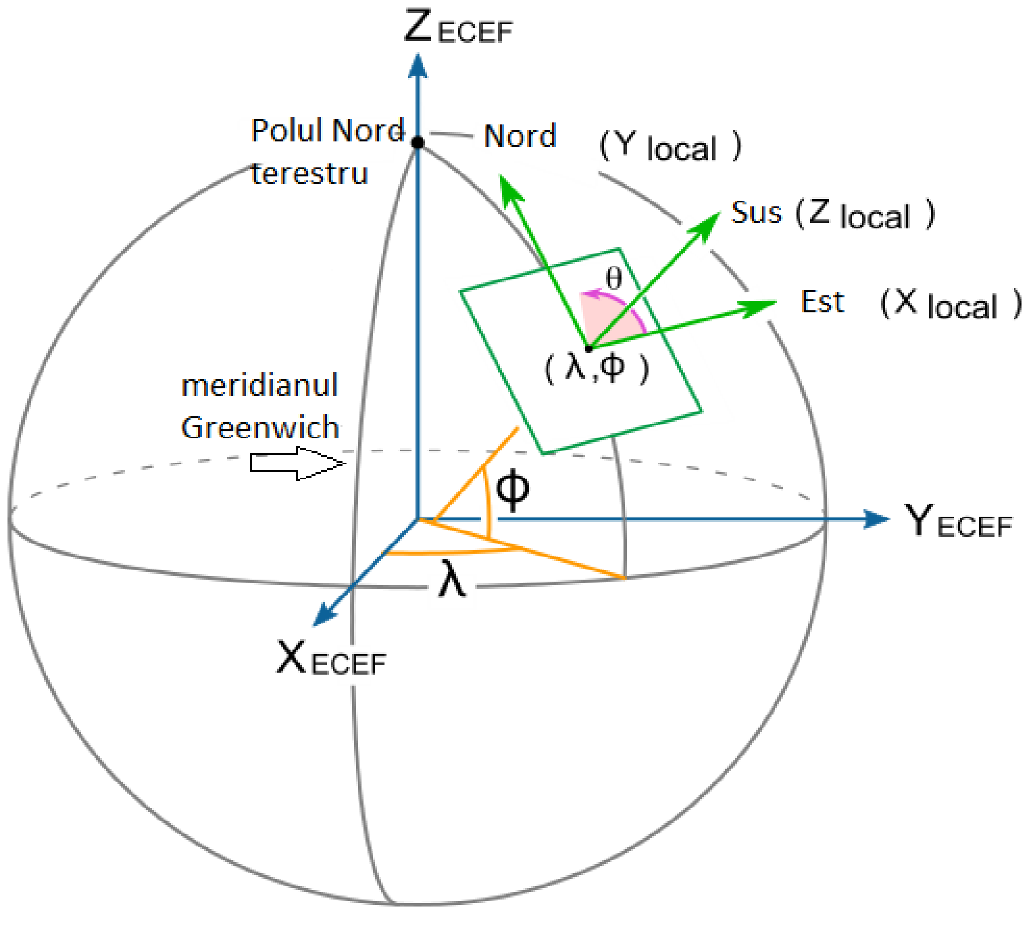

Classical Keplerian Elements (COE)

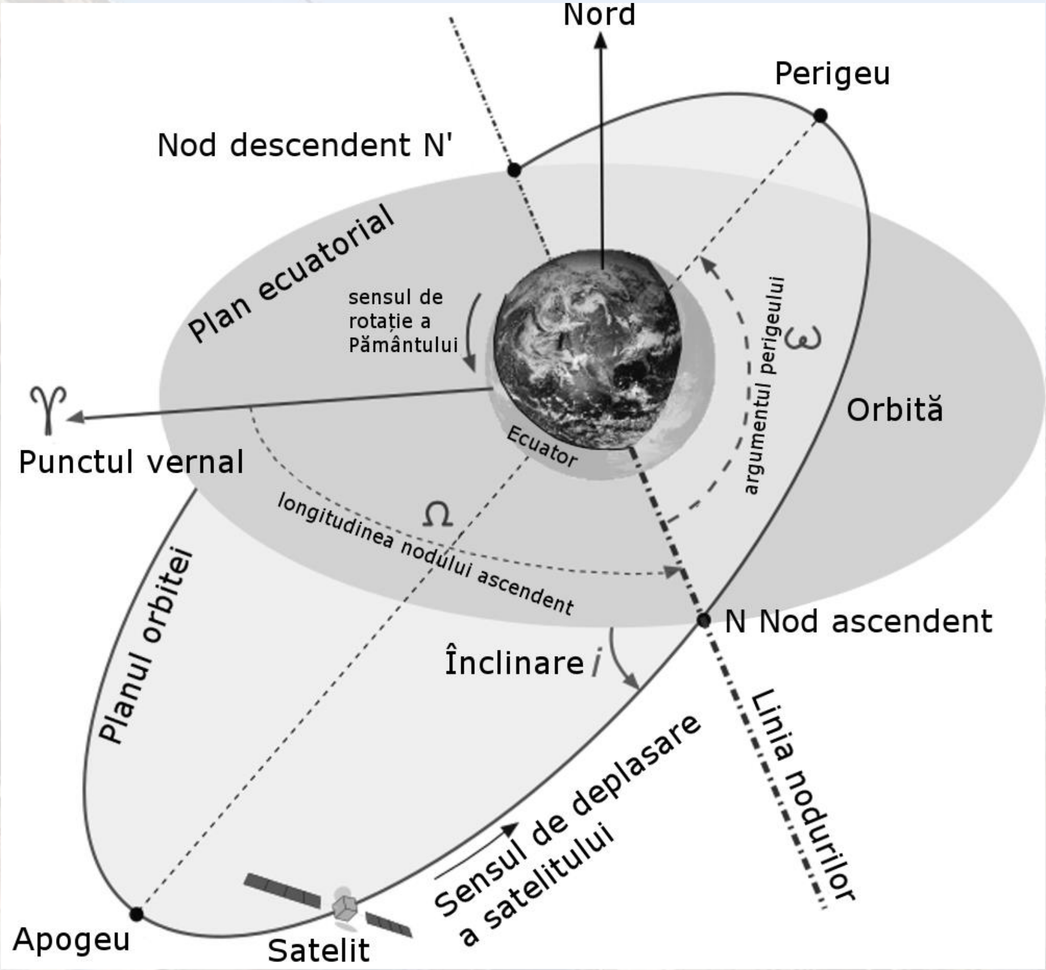

I. Shape and Size Parameters (2 elements: a and e)

Semi-major axis (a) – orbital size
Eccentricity (e) – orbital shape

II. Orbital Orientation Parameters (3 elements: i, Ω and ω)

Inclination (i) – angle with respect to the equatorial plane
Longitude of the Ascending Node (Ω or RAAN) – orientation of the orbital plane with respect to the vernal equinox
Argument of Perigee (ω) – position of perigee with respect to the ascending node

III. Position Parameter (1 element: M)

Mean Anomaly (M) – an angle that evolves linearly in time and describes the position of the satellite along its orbit

Dominant Orbital Perturbations in LEO

Perturbation	Effect	Consequence
J_2 - Earth's polar flattening (oblateness)	orbital plane precession	secular variations: nodal precession, apsidal precession
Atmospheric Drag	reduces and circularizes the orbit	orbital decay, followed by reentry

$$\vec{a}_{\text{tot}} = \underbrace{-\frac{\mu}{r^3}\vec{r}}_{\text{2-body}} + \underbrace{\vec{a}_{\text{drag}} + \vec{a}_{J_2}}_{\text{perturbații dominante LEO}}$$

Chapter 4: Physics of Atmospheric Reentry

Jules Verne, *Le Pays des fourrures* (1873):

- *"The sun, at its culmination, was completely obscured, and Lieutenant Hobson could no longer calculate the position of the island."*
- *"Without Sun, Moon, or stars, the instruments become useless, and the true position of the island cannot be determined."*
- Astronomer Thomas Black refuses to believe that the ephemerides are wrong: *"it is no longer where they think it is"*

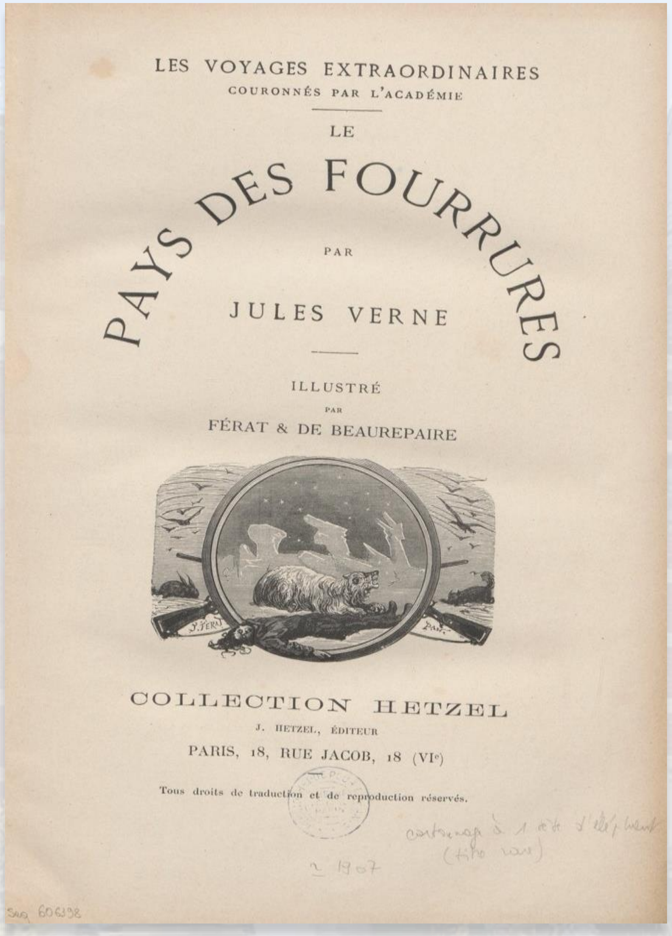
LES VOYAGES EXTRAORDINAIRES
COURONNÉS PAR L'ACADÉMIE
LE
PAYS DES FOURRURES
PAR
JULES VERNE
ILLUSTRÉ
PAR
FÉRAT & DE BEAUREPAIRE
COLLECTION HETZEL
J. HETZEL, ÉDITEUR
PARIS, 18, RUE JACOB, 18 (VIe)
Tous droits de traduction et de reproduction réservés.

Analogy:

- a passive object **(iceberg ↔ orbital debris)** in a dynamic environment **(ocean currents ↔ atmosphere)**, whose position is estimated through periodic observations
- the prediction of the event **(total eclipse ↔ reentry)** is accurate, but the position of the observer/object is affected by significant uncertainty
- the physical models are accurate, but the position remains constrained by environmental uncertainties: atmospheric density, aerodynamic drag, perturbations

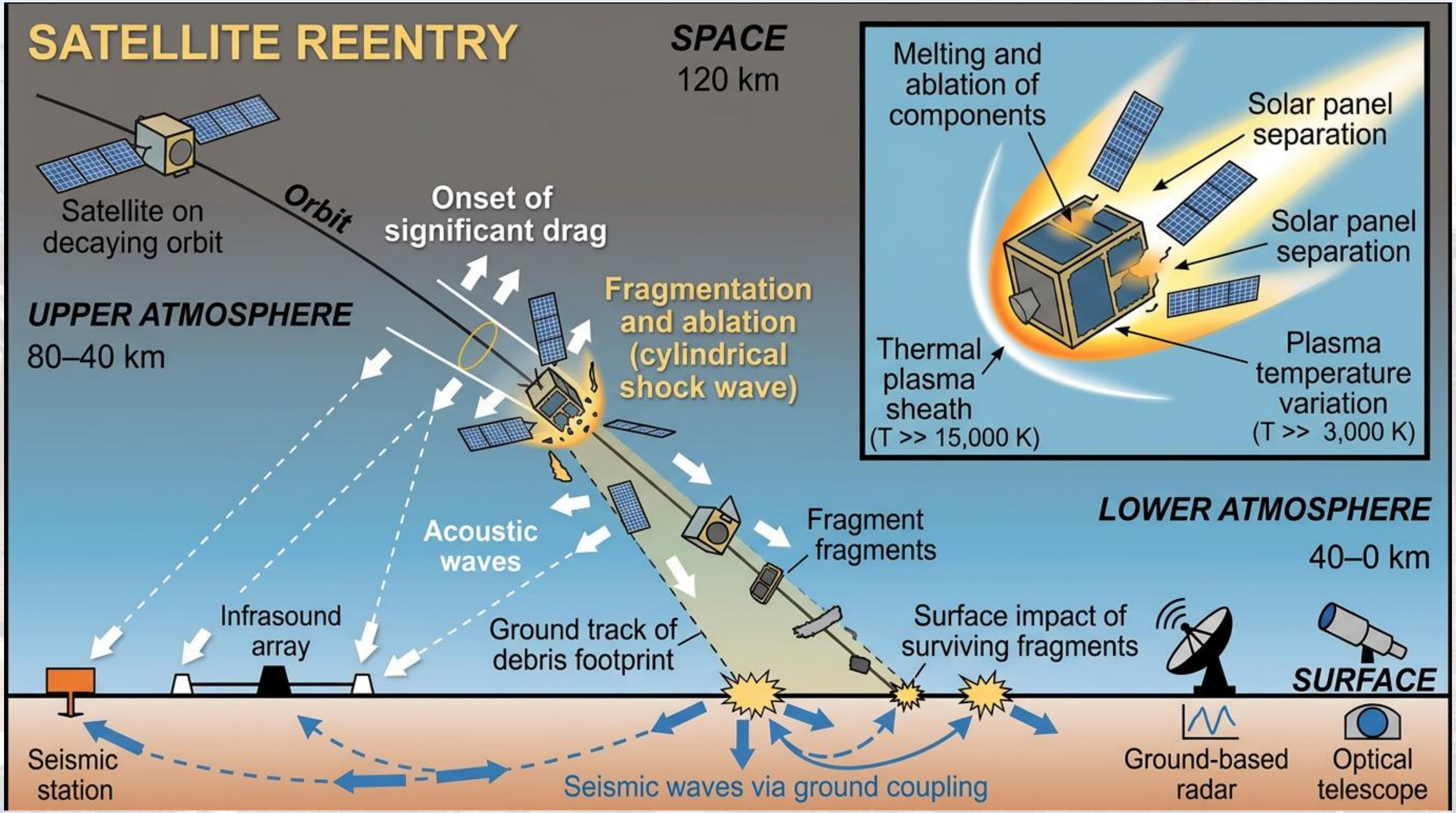
SATELLITE REENTRY
SPACE
120 km
Satellite on decaying orbit
Orbit
Onset of significant drag
UPPER ATMOSPHERE
80–40 km
Fragmentation and ablation (cylindrical shock wave)
Melting and ablation of components
Solar panel separation
Solar panel separation
Thermal plasma sheath
(T >> 15,000 K)
Plasma temperature variation
(T >> 3,000 K)
Acoustic waves
Fragment fragments
LOWER ATMOSPHERE
40–0 km
Infrasound array
Ground track of debris footprint
Surface impact of surviving fragments
SURFACE
Seismic station
Seismic waves via ground coupling
Ground-based radar
Optical telescope

I. Controlled Reentry of Starlink-1353

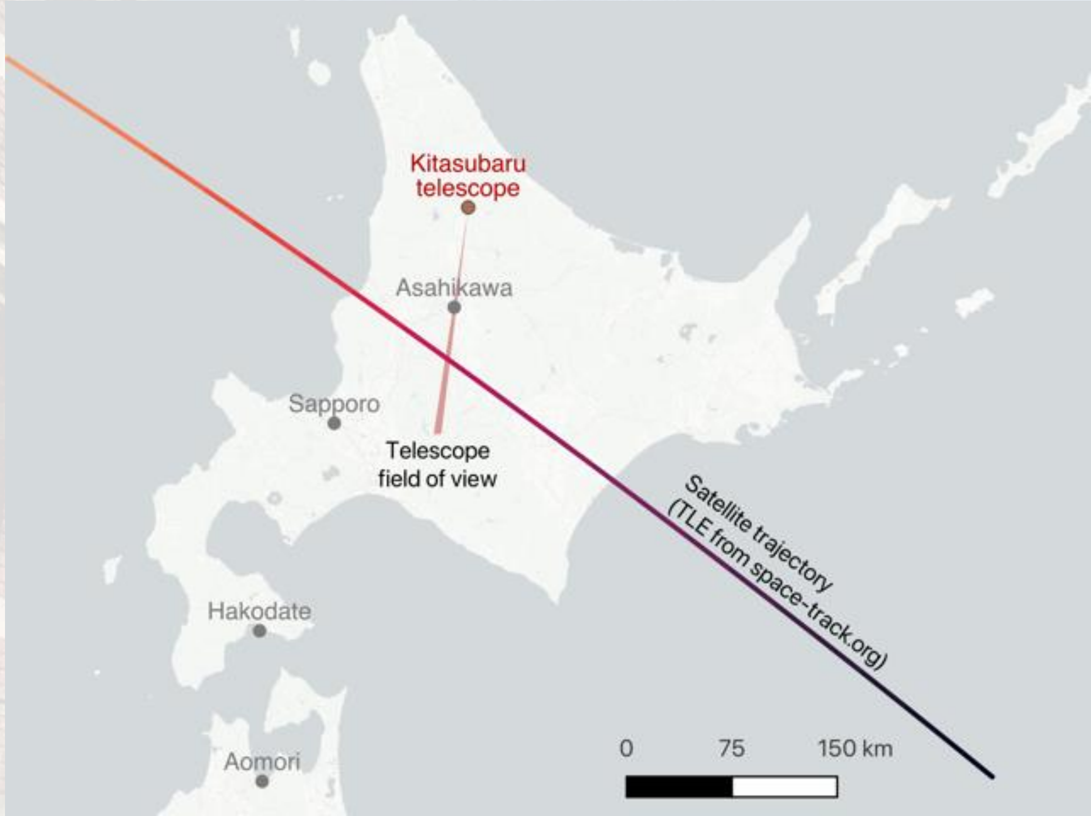

Event Timeline:

- first-generation satellite
- launched on 22 April 2020, but anomalies occurred during orbital insertion
- on 9 June 2020, it was declared non-functional by the operator SpaceX
- following deorbit maneuvers, on 21 February 2023 the satellite reentered the atmosphere
- the descent phase was captured by a telescope at the Kitasubaru Astronomical Observatory (Japan)

Aim

- hypothesis about the shape of the Starlink-1353 satellite and the mass distribution of the internal components
- approximation of the number of fragments, composition and their mass upon re-entry phase

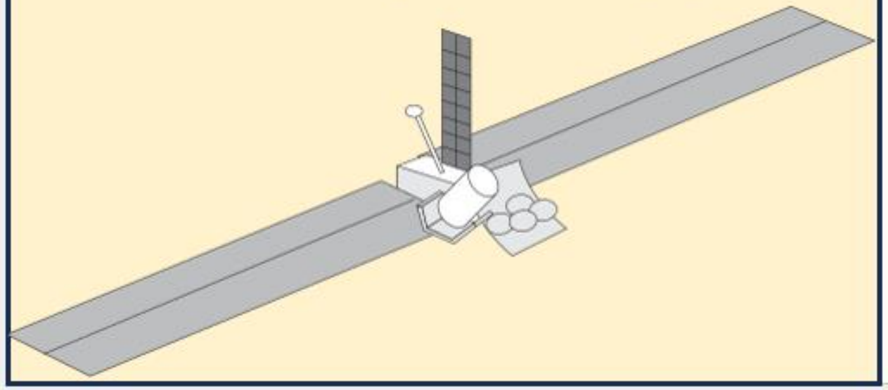

Methods

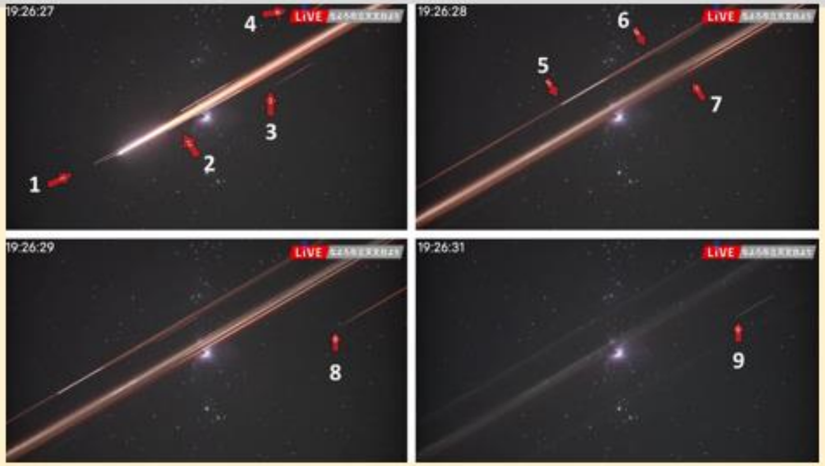

- visual frame by frame analysis
- simulations with DAS for plausible and non-plausible scenarios
- dynamical behaviour before the moment of planned re-entry

Universitatea din București
Virtute et Sapientia

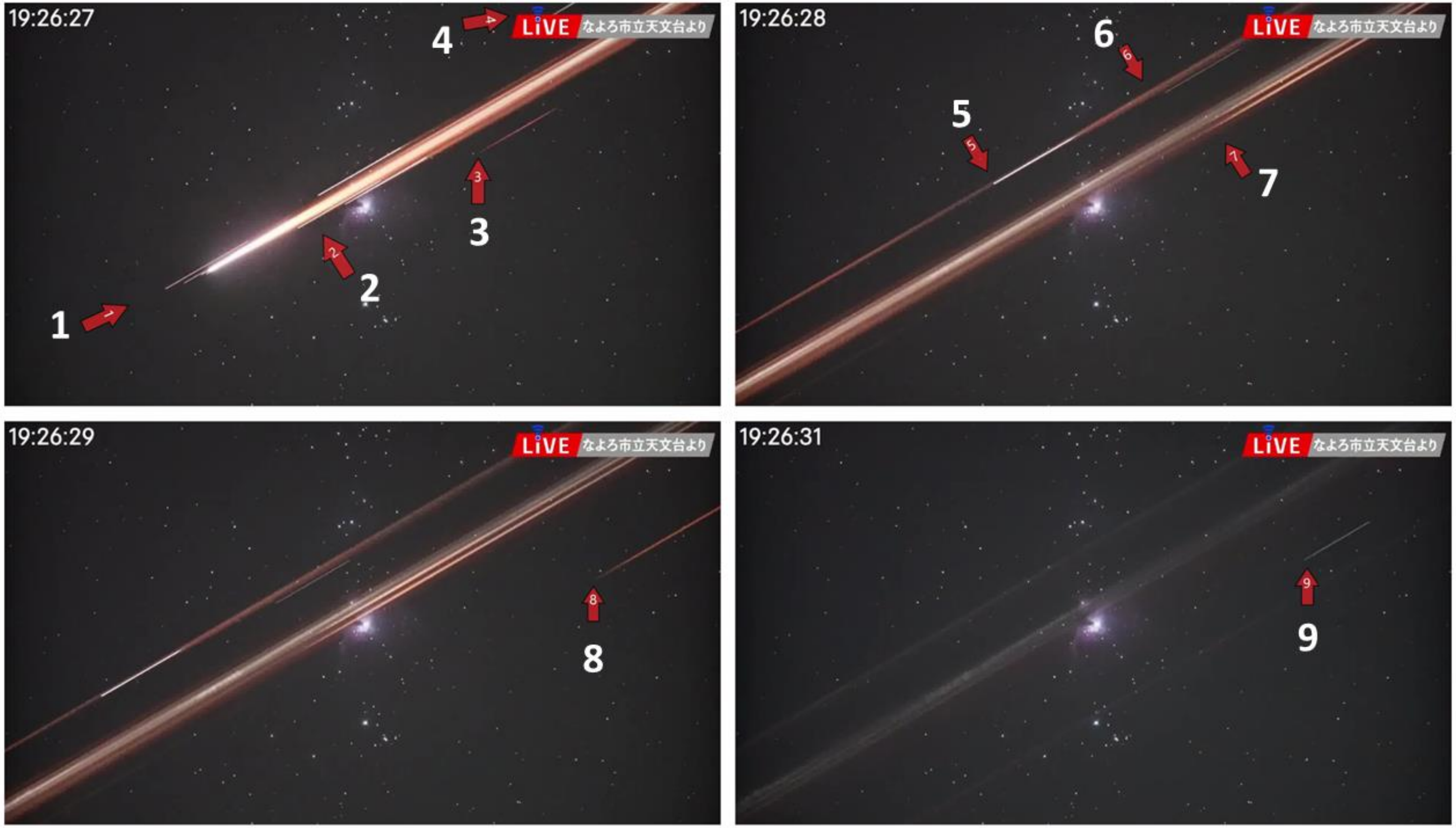

Frame-by-frame analysis

15 fragments were identified following the breakup of the main body:

- arrow 1 => 4 fragments
- arrow 2 => 3 fragments
- arrow 3 => 1 fragment
- arrow 4 => 1 fragment
- arrow 5 => 1 fragment
- arrow 6 => 1 fragment
- arrow 7 => 2 fragments
- arrow 8 => 1 fragment
- arrow 9 => 1 fragment

Estimation of the mass distribution of the Starlink-1353 satellite components

Generic component	Number of items	Generic materials	Min. - Max. mass per unit [kg]	Probability of hitting Earth	Potential residuals
Solar panel	1	aluminium alloy silicium	70 - 100	0	alumina
Satellite body	1	aluminum alloy	90 - 130	0	alumina
Thruster internals	1	iron	3 - 1.5	high	iron
Ion thruster	1	aluminum alloy graphite tungsten/ tantali	7 - 2.5	high	alumina graphite tungsten/ tantali
Reaction wheel	4	stainless steel	1 - 0.25	high	stainless steel
Comms. components	4	silicon carbide	1 - 0.25	high	silicon carbide
Comms. antenna	2	aluminium alloy	1 - 0.25	low	alumina
Li-Ion batteries	4	aluminium alloy silicium / iron	18 - 5	high	alumina iron
Onboard electronics	1	aluminum alloy FR4 / tantali silicium / tungsten	3 - 1.5	medium	alumina tantali tungsten
Stacking racks	3	Inconel	1 - 0.33	medium	stainless steel/ alumina
Fastening systems	1	Inconel	1 - 0.5	medium	stainless steel/ alumina
Cables	1	cooper alloy aluminium alloy	1 - 0.5	0	alumina

Plausible Scenario

Generic component	Number of items	Generic material	Demise Alt [km]	Total DCA [sq m]
Root Object	1	Aluminum (generic)	0	15.12
Solar panel	1	Aluminum (generic)	**14.5**	0
Satellite body	1	Aluminum (generic)	**64.4**	0
Thruster internals	1	Iron	0	0.38
Reaction wheel	4	Stainless Steel (generic)	0	2.38
Comms comp	4	Silicon Carbide	0	1.98
Comms antenna	2	Aluminum (generic)	0	2.18
Li-ion batteries	4	Aluminum (generic)	0	4.4
OnBoard electronics	1	Aluminum (generic)	0	0.99
Ion thruster	1	Tungsten	0	0.6
Stacking racks	3	Inconel 600	0	1.79
Fastening systems	1	Inconel 600	0	0.43
Cables	1	Copper Alloy	**50.9**	0

Non-Plausible Scenario

Generic component	Number of items	Generic material	Demise Alt [km]	Total DCA [sq m]
Root Object	1	Aluminum (generic)	0	9.62
Solar panel	1	Aluminum (generic)	0	0.52
Satellite body	1	Aluminum (generic)	0	9.1
Thruster internals	1	Iron	0	0
Reaction wheel	4	Stainless Steel (generic)	0	0
Comms comp	4	Silicon Carbide	0	0
Comms antenna	2	Aluminum (generic)	0	0
Li-ion batteries	4	Aluminum (generic)	0	0
OnBoard electronics	1	Aluminum (generic)	0	0
Ion thruster	1	Tungsten	0	0
Stacking racks	3	Inconel 600	0	0
Fastening systems	1	Inconel 600	0	0
Cables	1	Copper Alloy	0	0

Credit: The data were obtained based on simulations using Debris Assessment Software (DAS)

II. Uncontrolled Reentry of the ERS-2 Satellite

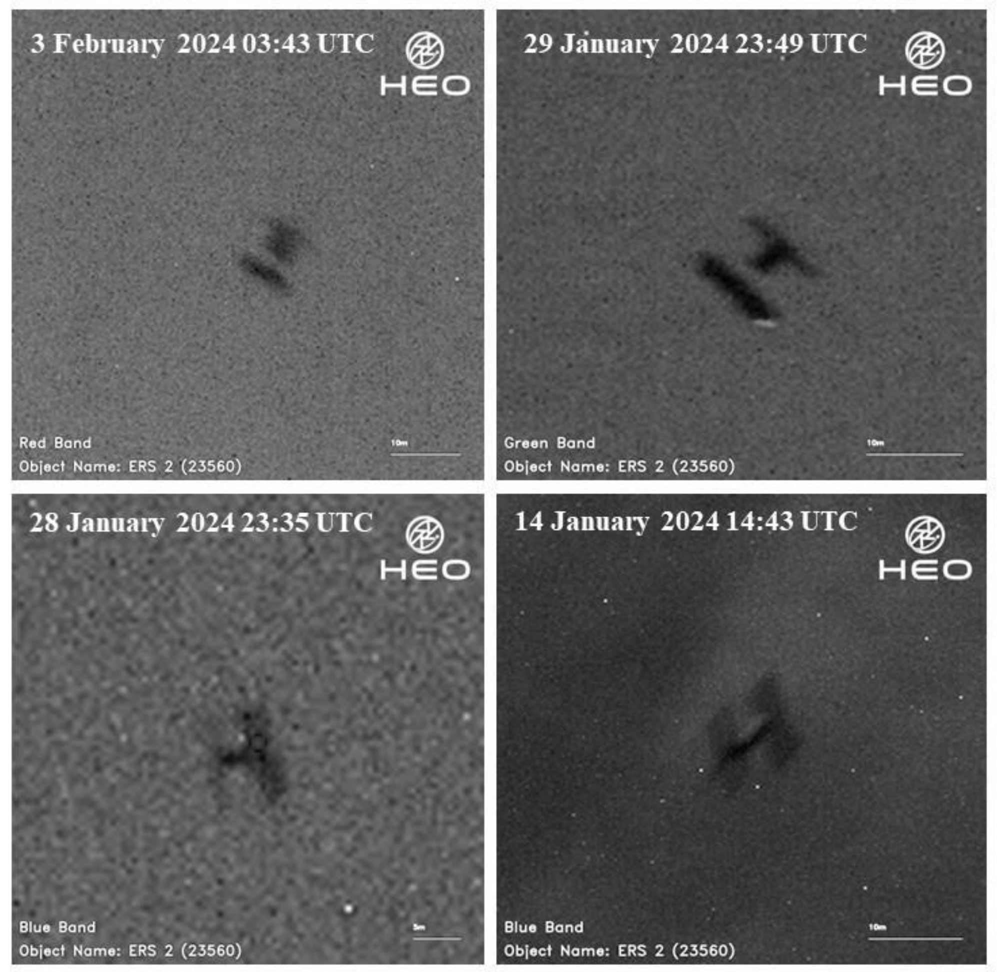

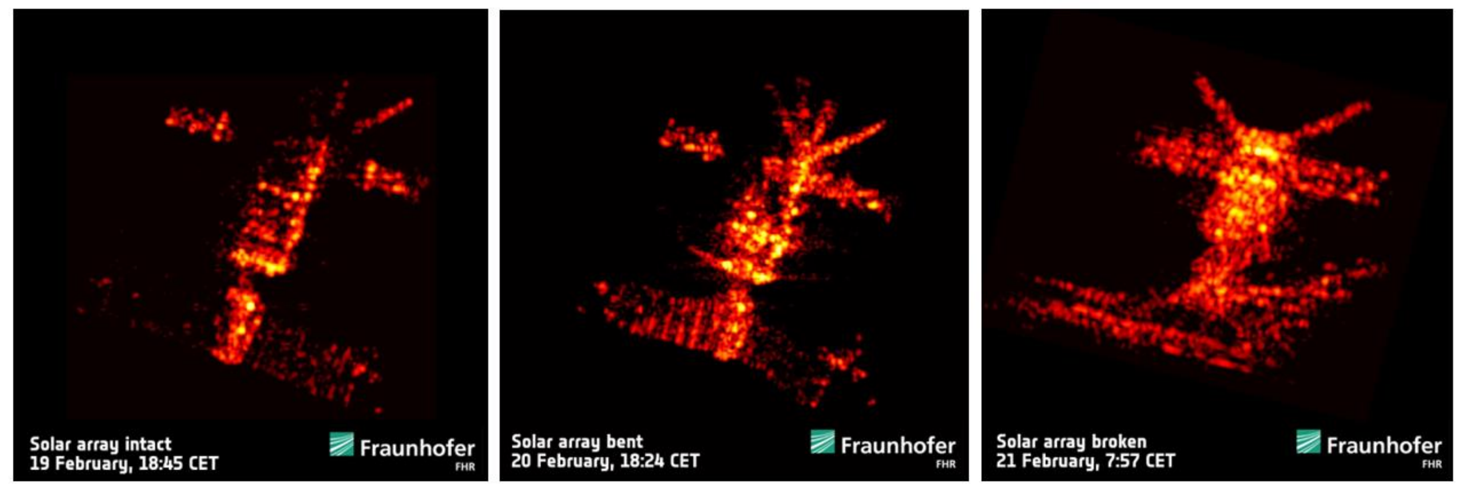

- launched on 21 April 1995
- on 21 February 2024, it reentered the atmosphere in an uncontrolled manner, and the fragments were scattered over the North Pacific Ocean

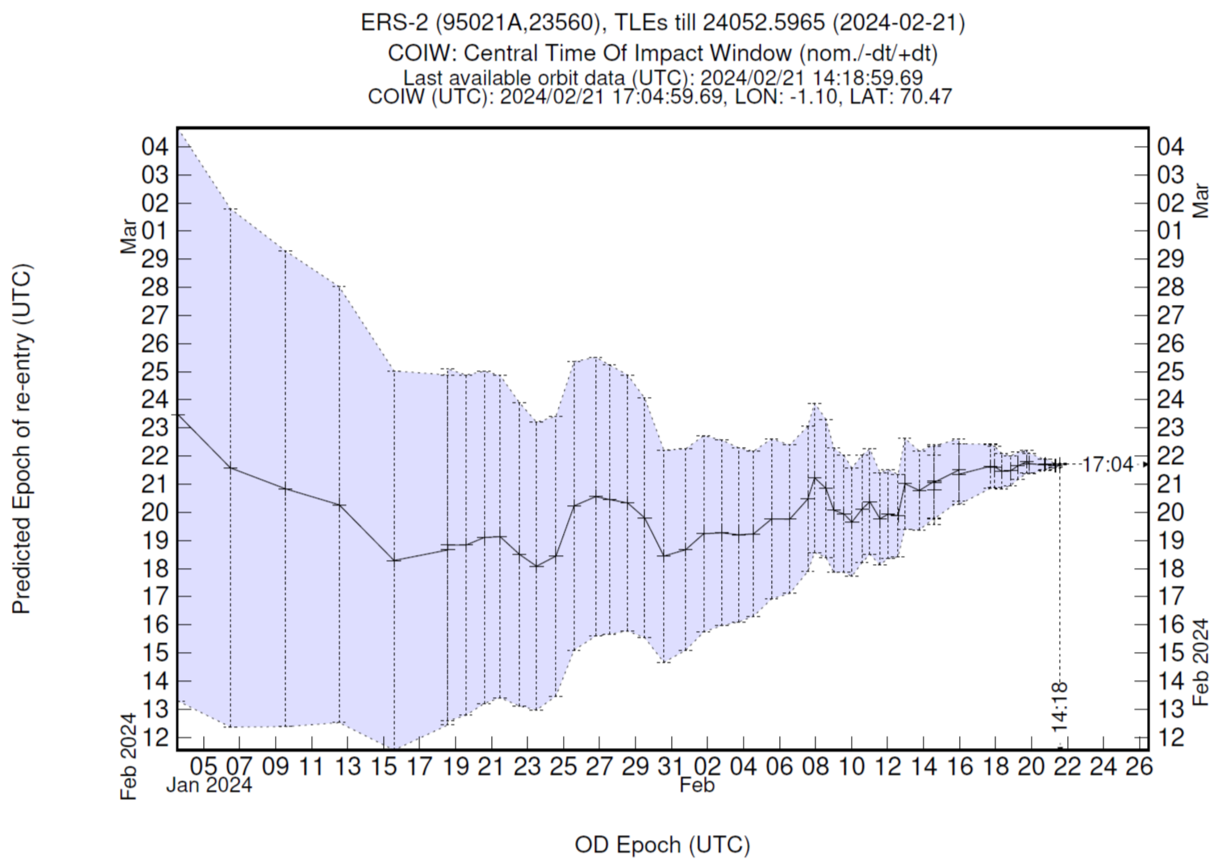
ERS-2 (95021A,23560), TLEs till 24052.5965 (2024-02-21)
COIW: Central Time Of Impact Window (nom./-dt/+dt)
Last available orbit data (UTC): 2024/02/21 14:18:59.69
COIW (UTC): 2024/02/21 17:04:59.69, LON: -1.10, LAT: 70.47
Predicted Epoch of re-entry (UTC)
OD Epoch (UTC)
Feb 2024
Mar
Jan 2024
Feb
17:04
14:18

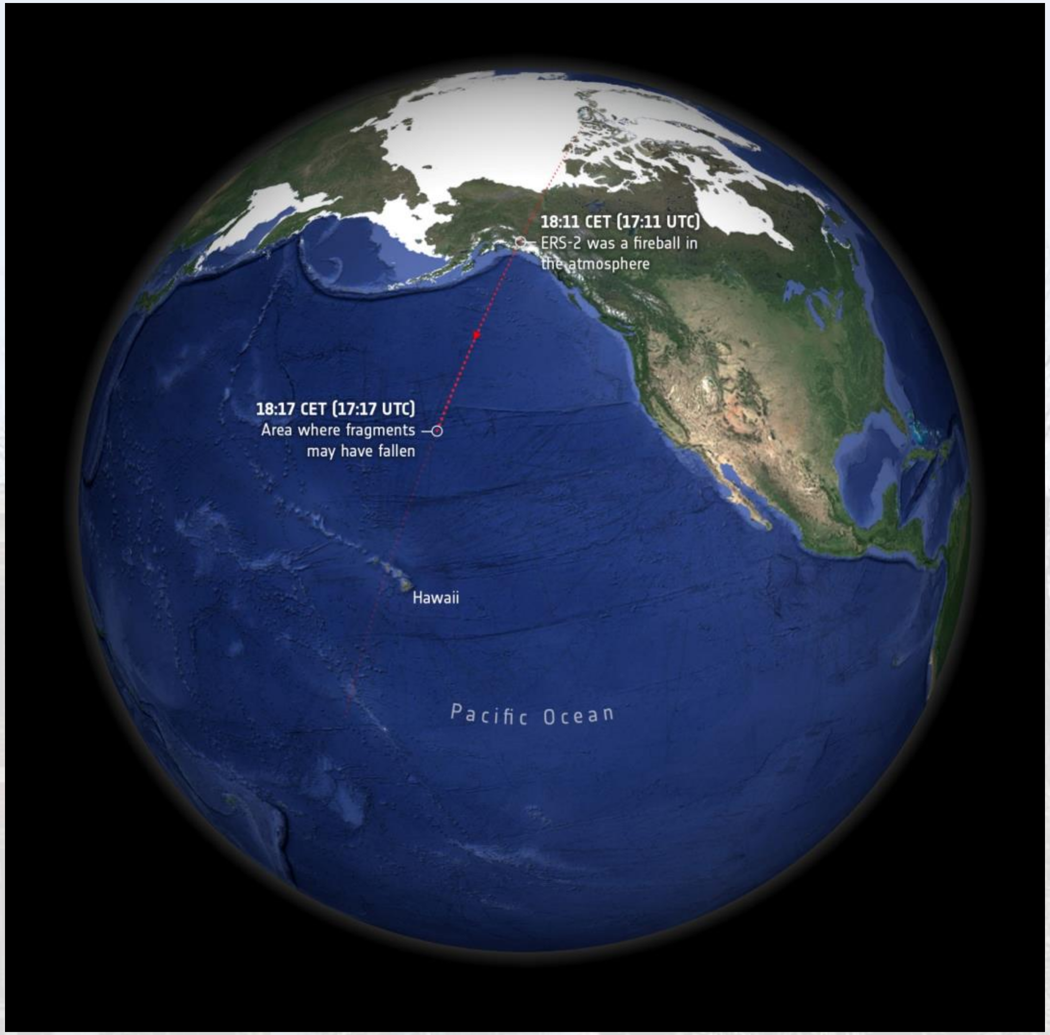
18:11 CET (17:11 UTC)
ERS-2 was a fireball in the atmosphere
18:17 CET (17:17 UTC)
Area where fragments may have fallen
Hawaii
Pacific Ocean

Reentry Simulations

a) Debris Assessment Software (DAS) developed by National Aeronautics and Space Administration (NASA)

Table 3

Estimation of demise altitude and total DCA for the first scenario

Generic component	Number of items	Generic material	Demise Alt [km]	Total DCA [sq m]
Root Object	1	Aluminum (generic)	0	63.12
Central body	1	Aluminum (generic)	0	9.68
Antennas	1	Aluminum (generic)	0	14.67
Solar pannels	2	Fiberglass	0	38.76

b) Debris Risk Assessment and Mitigation Analysis (DRAMA) developed by European Space Agency (ESA)

- Input mode: Expert / Re-entry and Risk
- Re-entry type: uncontrolled
- Orbital states: the last TLE
- Satellite attitude: tumbling
- Environment dynamic NRLMSISE-00 with density scaling factor 1.0
- Solar flux 164 sfu (February 21, 2024) / Casualty threshold: 15 J

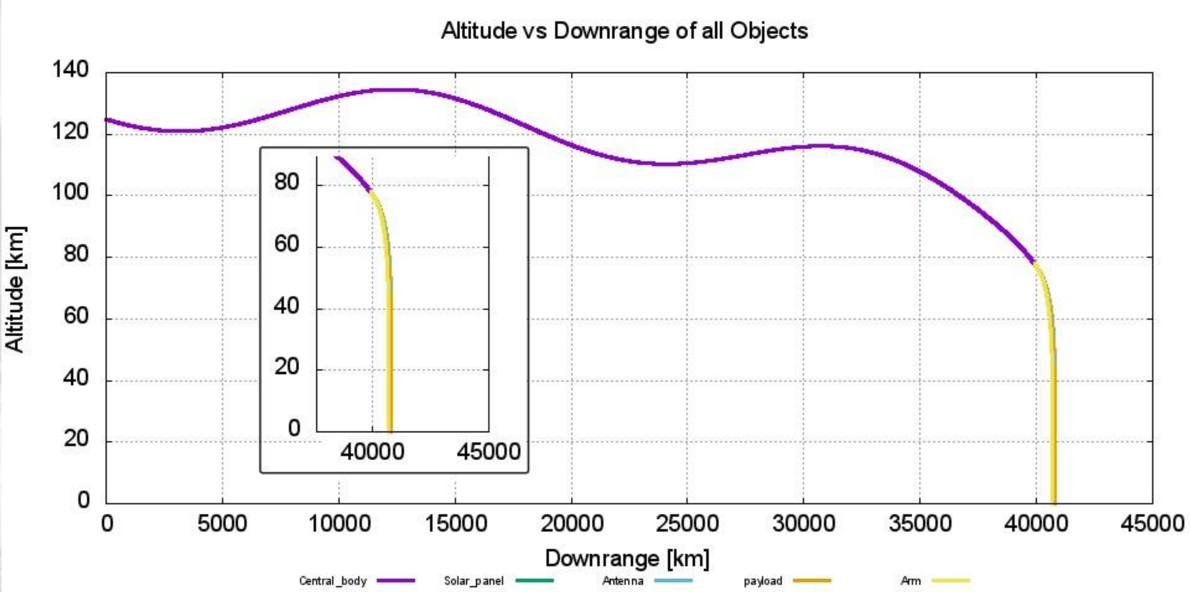

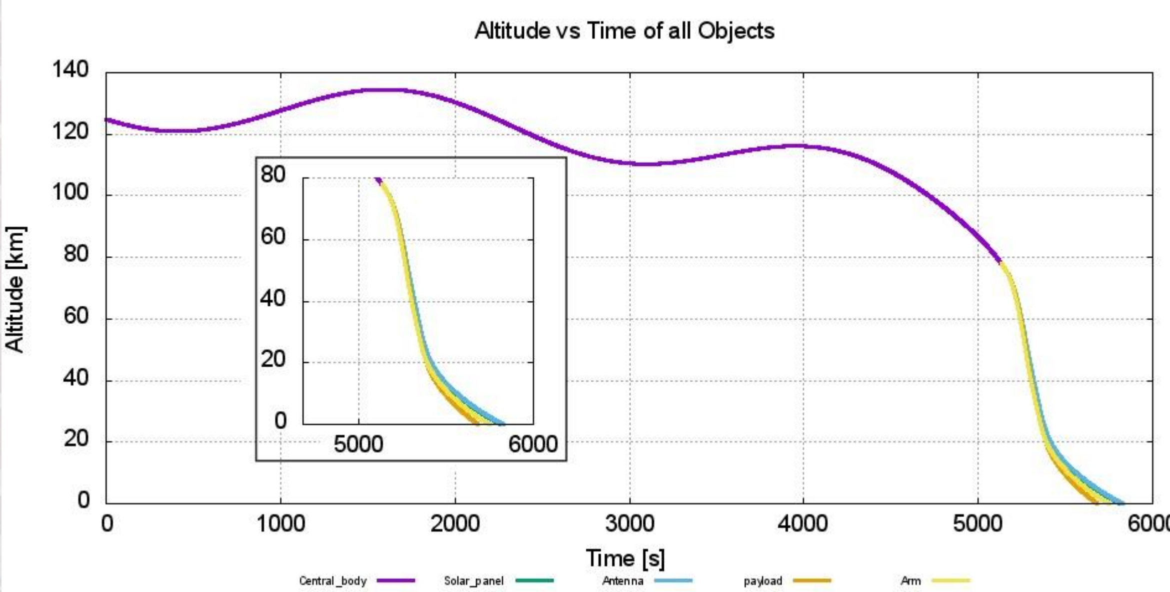

c) DEBRISK developed by Centre National d'Études Spatiales (CNES)

- Input mode: Expert / Re-entry and Risk
- Re-entry type: uncontrolled
- Orbital states: the last TLE
- Satellite attitude: tumbling
- Environment dynamic NRLMSISE-00 with density scaling factor 1.0
- Solar flux 164 sfu (February 21, 2024) / Casualty threshold: 15 J

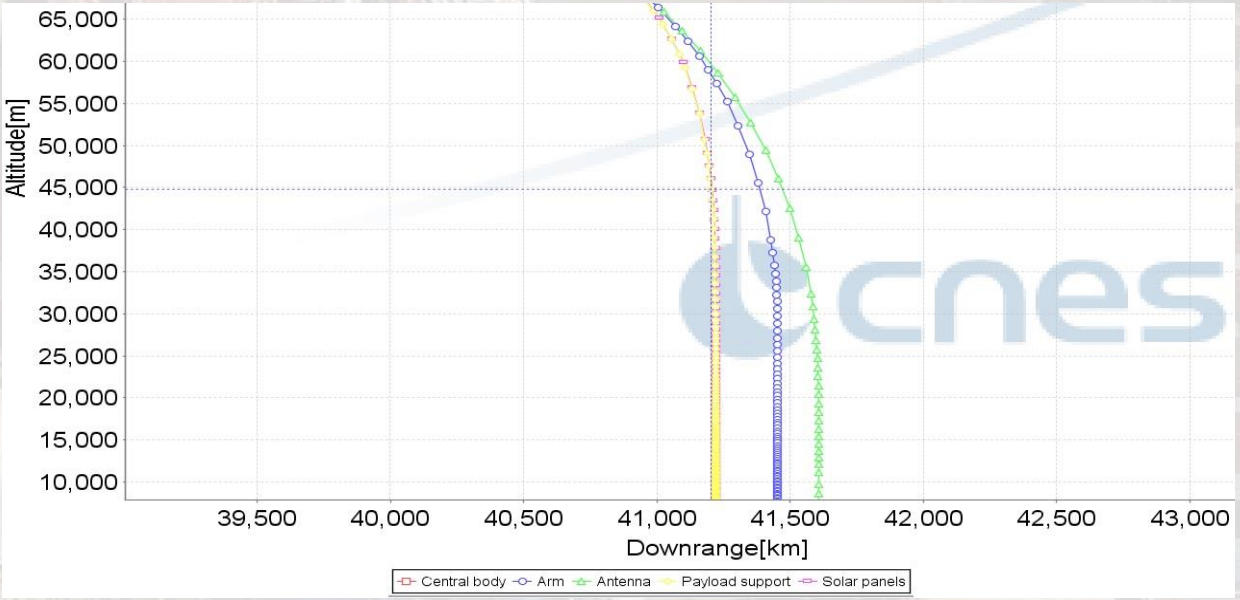

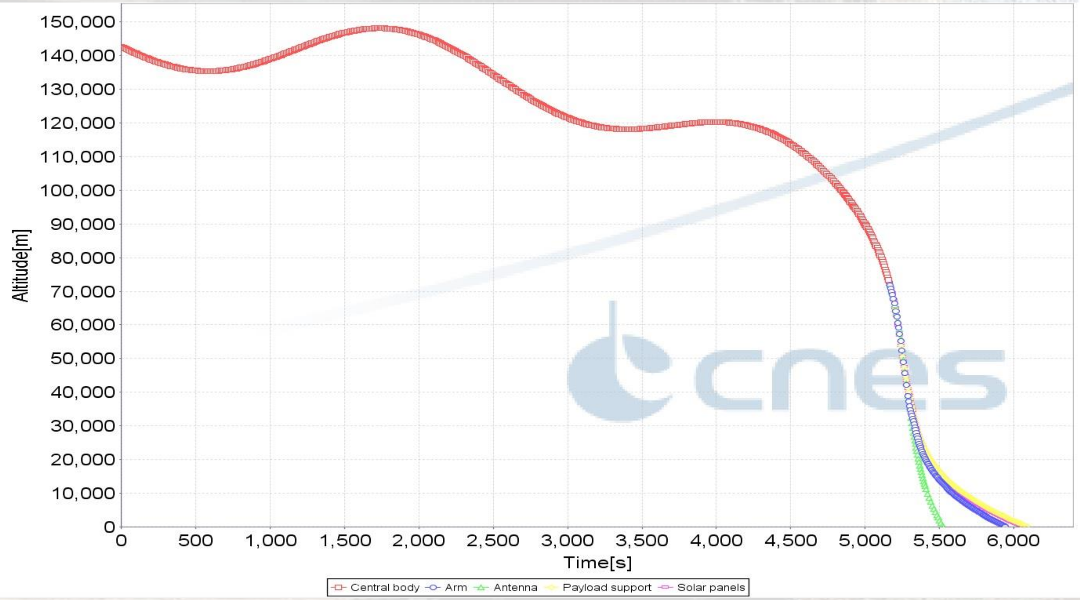

Chapter 5: Impact on Observational Astronomy

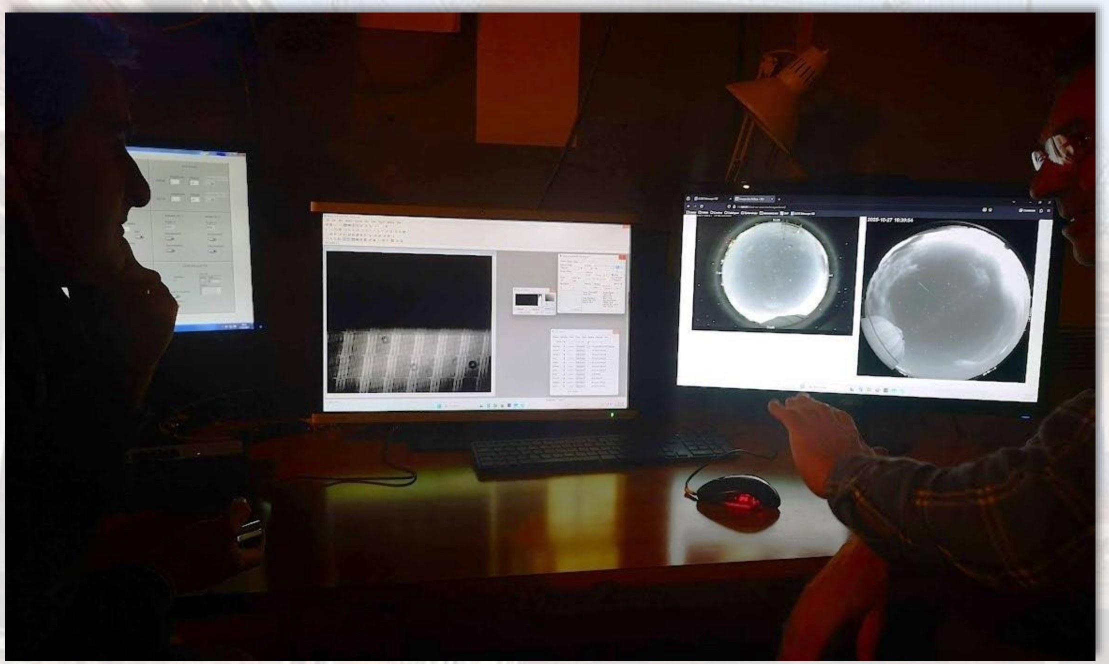

ML

NO

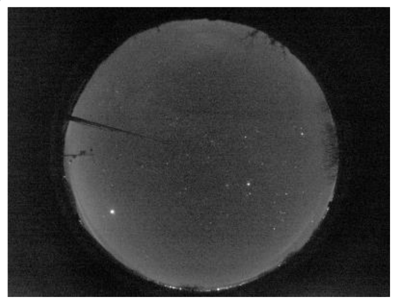

Scientific Data Processing Pipeline

YES

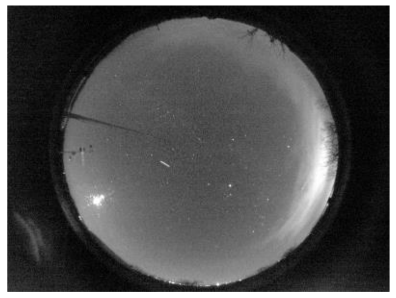

SST Monitoring Pipeline

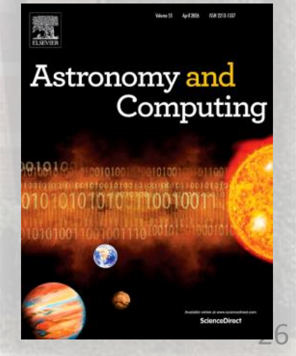

Image Acquisition

Berthelot Observatory (IAU Code L54)

All-sky camera:
4.9 x 3.6 mm Sony CCD chip ICX445
(1296 x 966 active pixels, 12 bit)

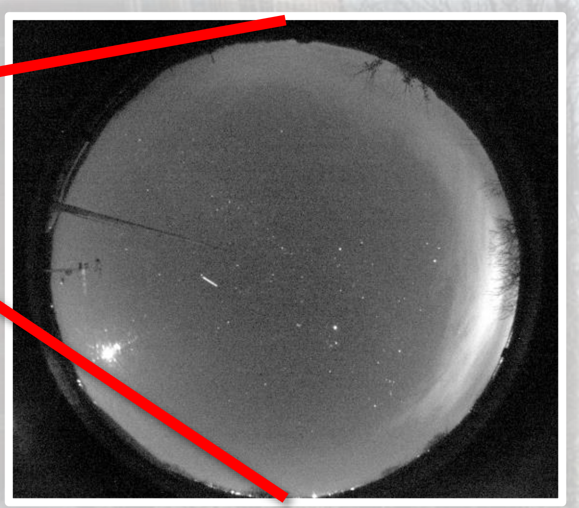

Data Preprocessing

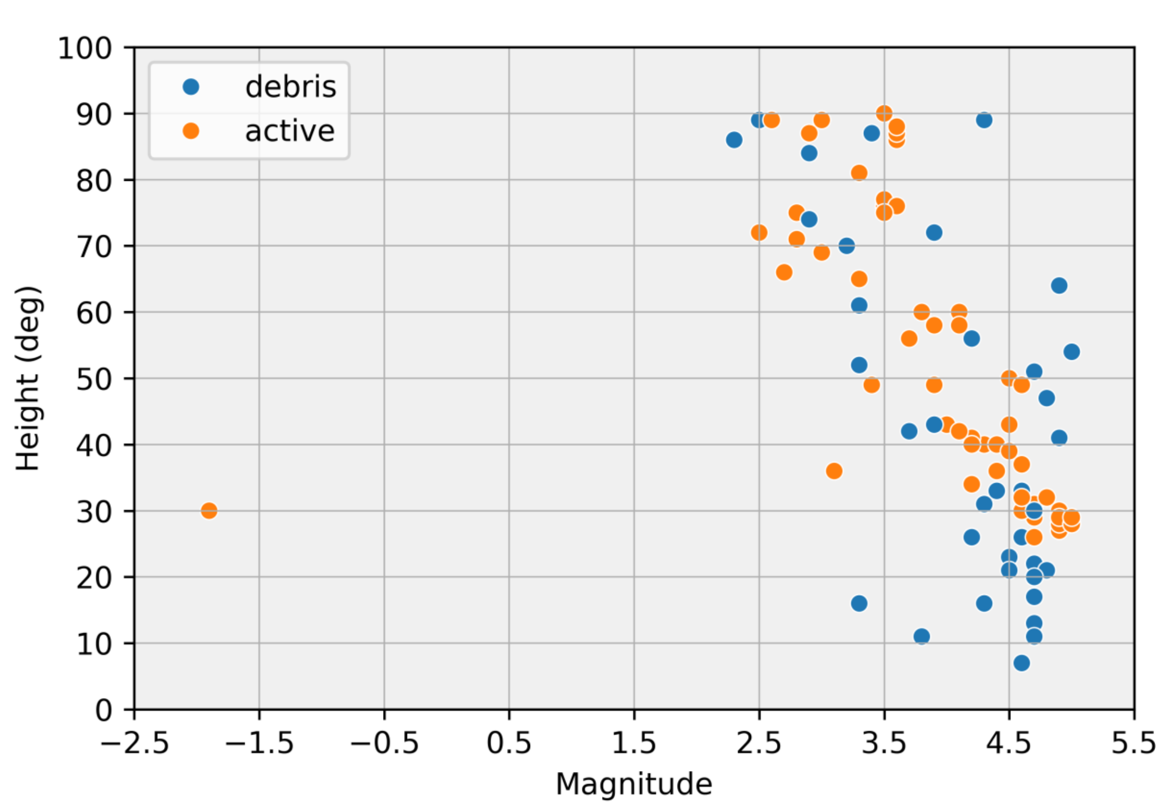

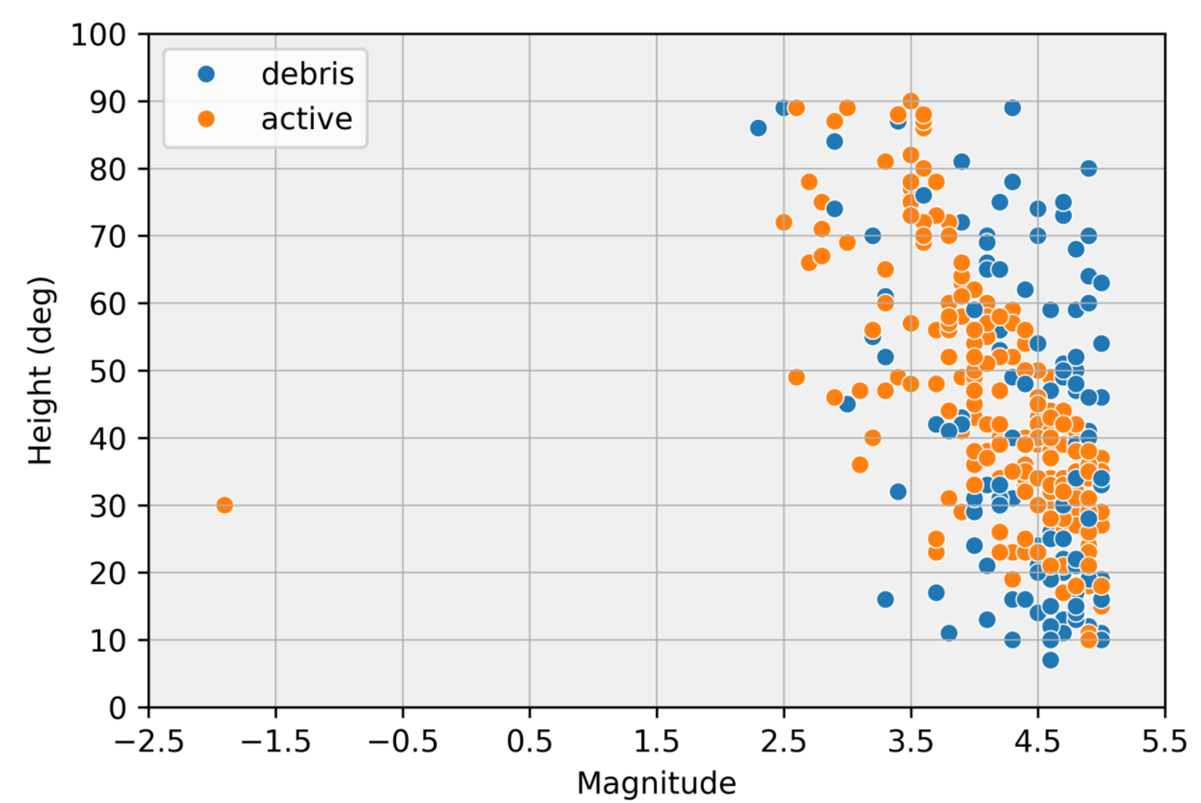

Phase 1: 1,589 FITS images acquired from 96 transits: 59 satellites and 37 orbital debris objects

Phase 2: 8,596 FITS images acquired from 358 transits: 224 satellites and 134 orbital debris objects

Data Preprocessing

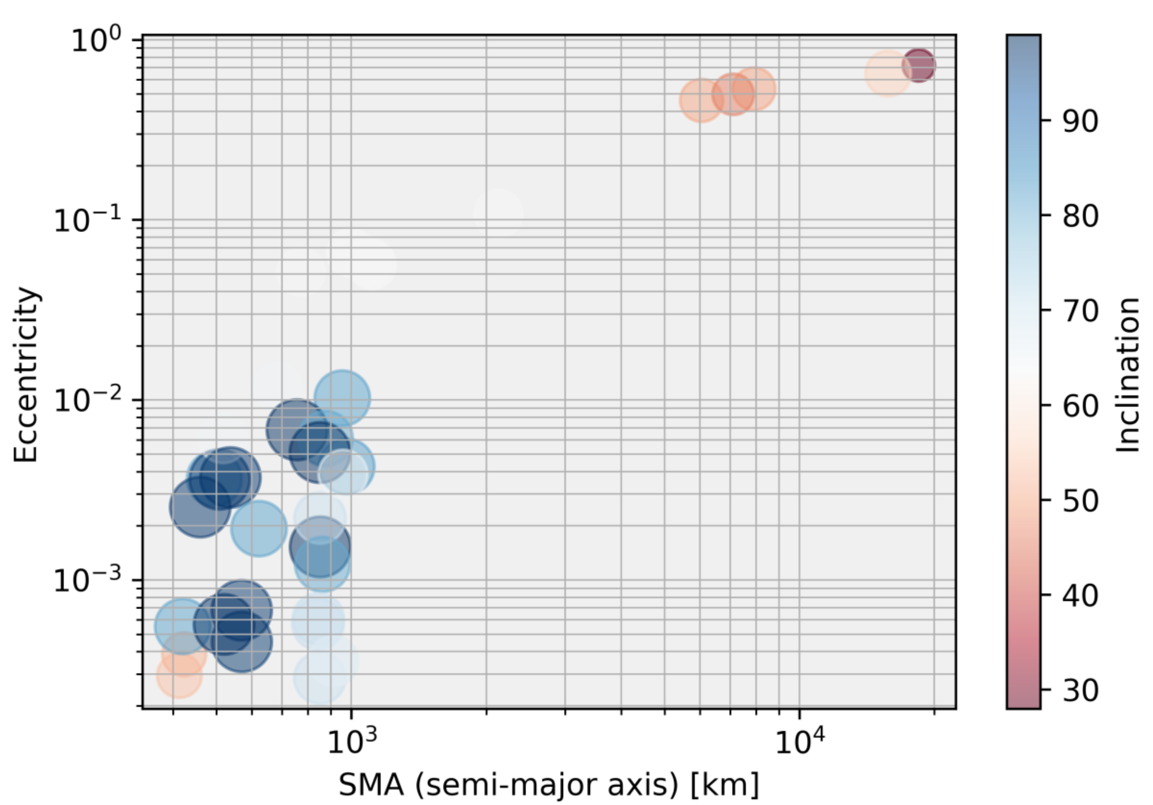

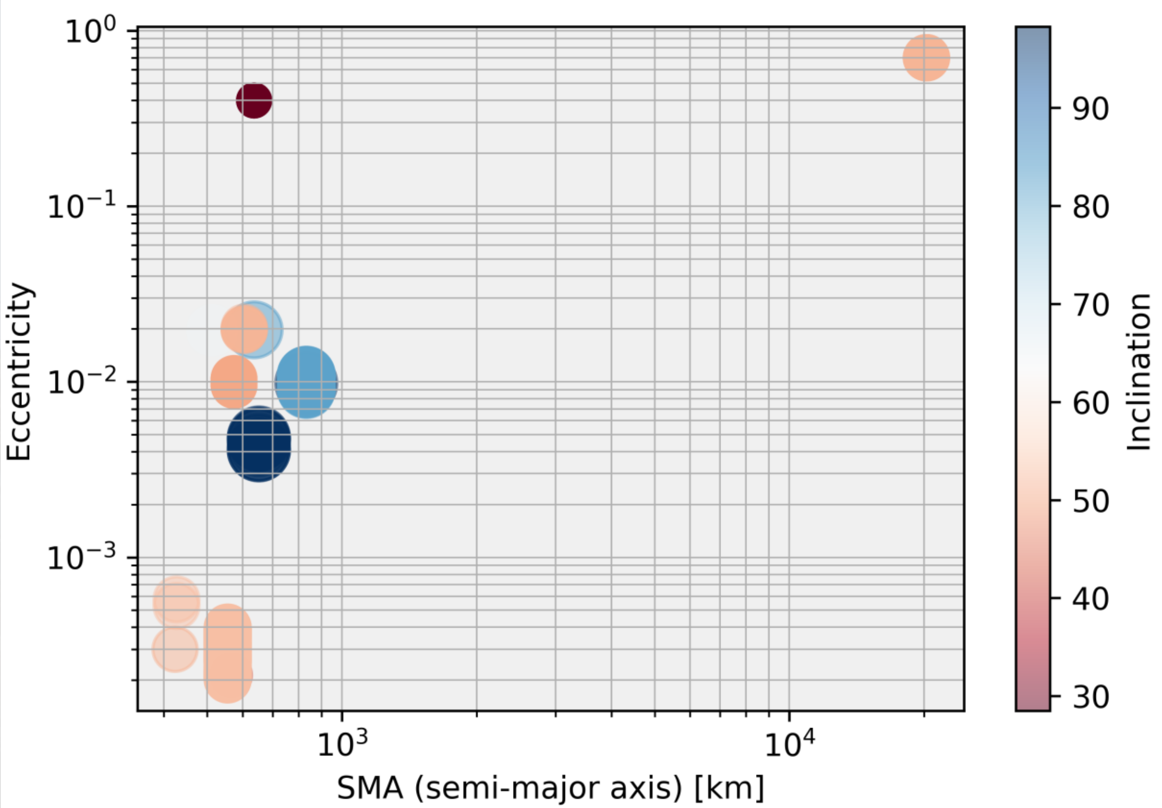

Phase 1: 1,589 FITS images acquired from 96 transits: 59 satellites and 37 orbital debris objects

Phase 2: 8,596 FITS images acquired from 358 transits: 224 satellites and 134 orbital debris objects

1411 Total Images

View All Images →

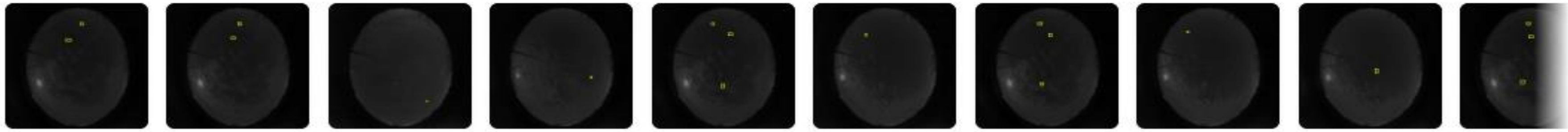

Dataset Split

TRAIN SET 70%	VALID SET 20%	TEST SET 10%
988 Images	282 Images	141 Images

Phase 1

Phase 2

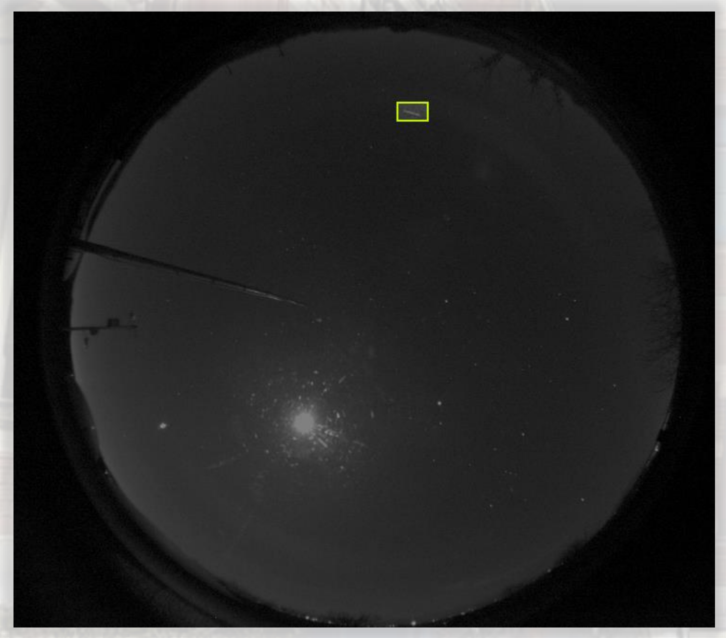

13162 Total Images

View All Images →

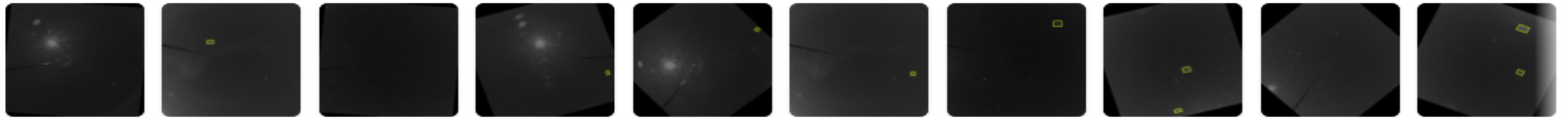

Dataset Split

TRAIN SET 82%	VALID SET 11%	TEST SET 7%
10736 Images	1454 Images	972 Images

Preprocessing

Auto-Orient: Applied
Resize: Fill (with center crop) in 640x640
Grayscale: Applied

Augmentations

Outputs per training example: 2
Flip: Horizontal, Vertical
Rotation: Between -45° and +45°

Results

TP (True Positive) = 0,91

TN (True Negative) = 1

FP (False Positive) = 0

FN (False Negative) = 0,09

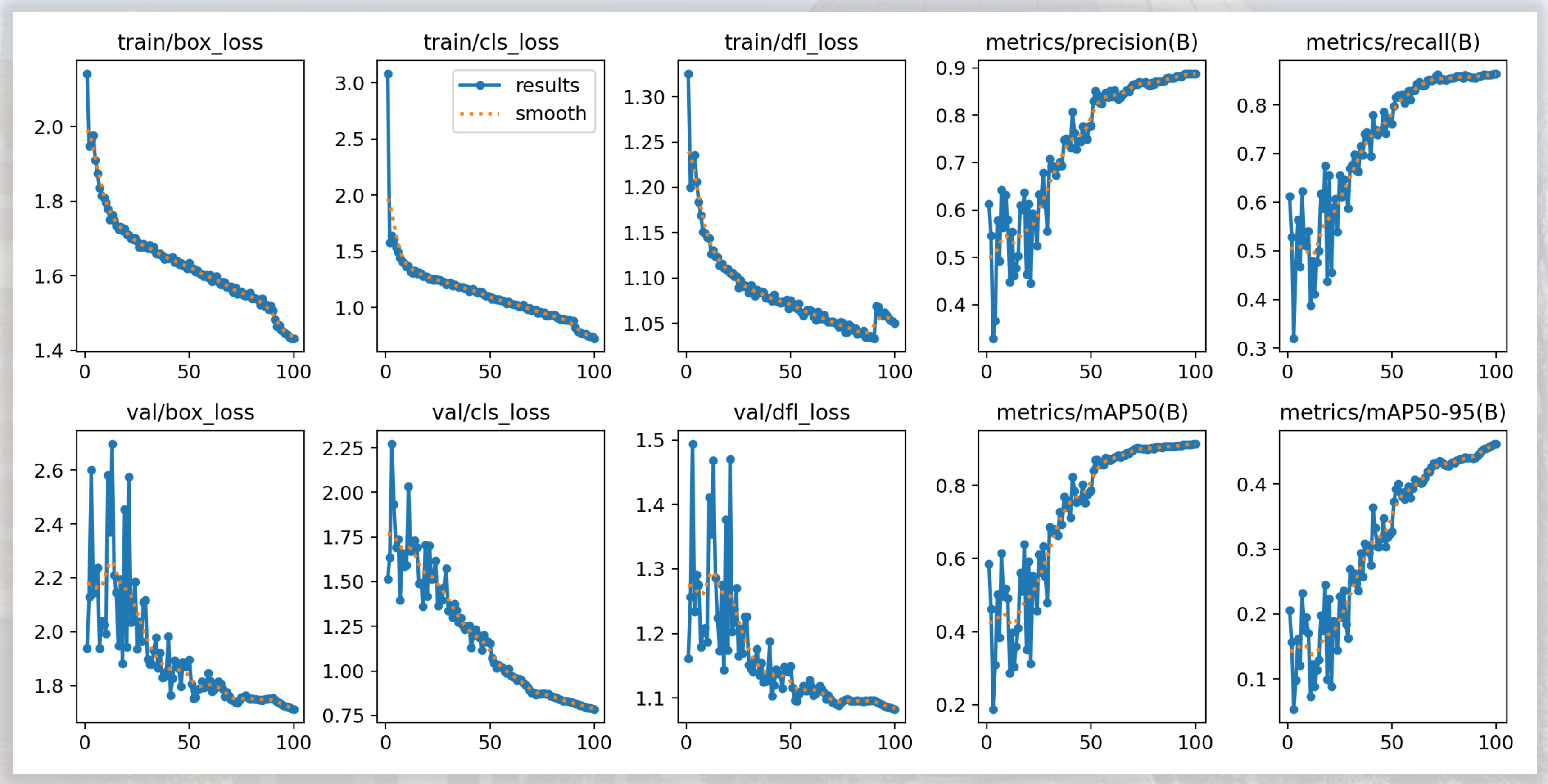

Performance Metrics:

Accuracy = 95,5%

Precision = 100%

Recall = 91%

(only 9% of the trails were missed)

Predictions on the Test Set

- the system is not affected by clouds or light pollution
- multiple trails detected in images
- images with no trails detected

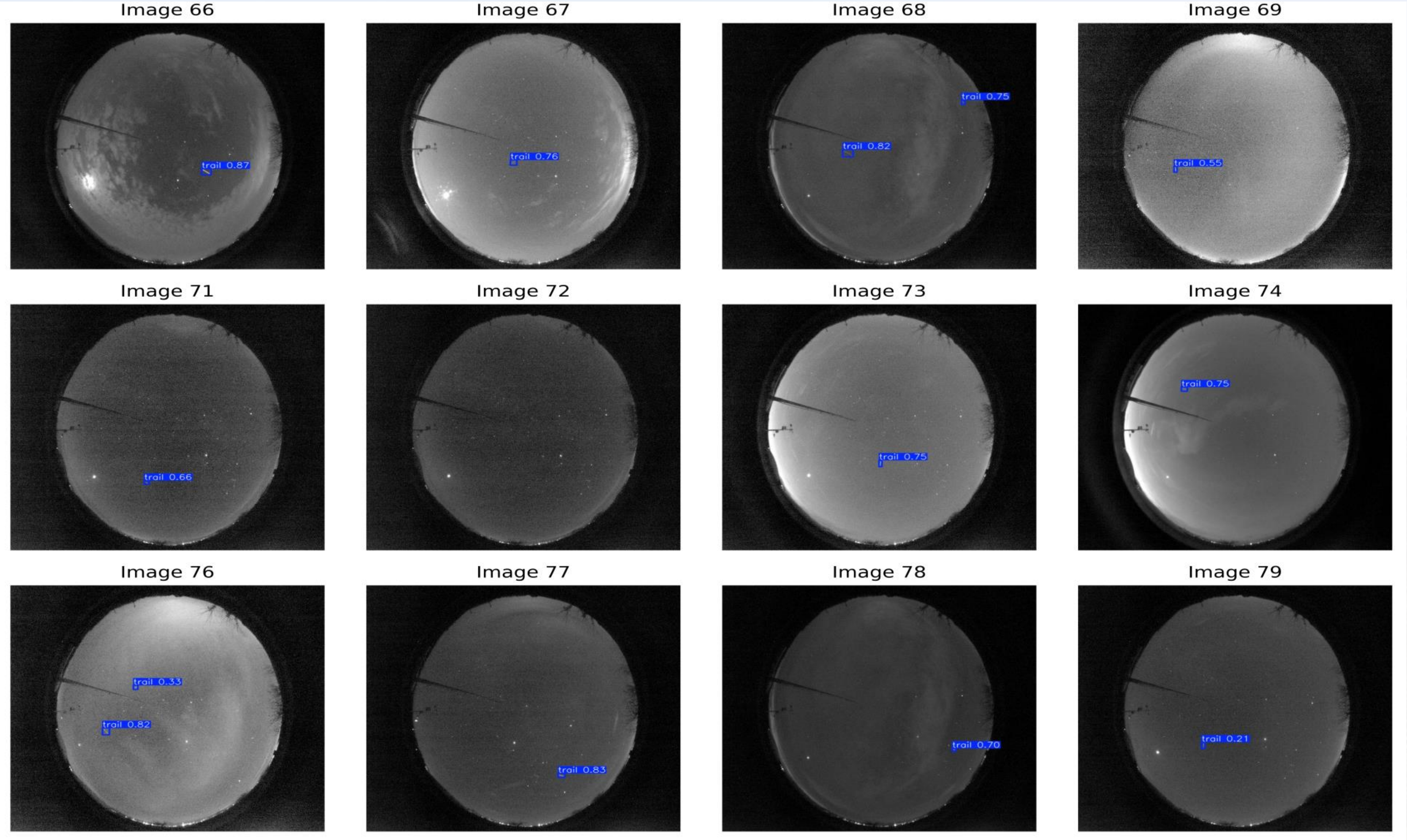

Conclusions

BALANCE IN INNOVATION

- launch cost optimization
- environmental factors and sustainability
- compliance with stricter technical regulations

GLOBAL HARMONIZATION

- dynamic allocation of orbital slots and insertion licenses
- mandatory EOL deorbit plans
- common international standards

LEGAL FRAMEWORK

- inadequate in the current context
- urgent revision of the *Outer Space Treaty*, ratified and in use since 1967

ORBITAL DEBRIS REMOVAL

- ADR: experimentally demonstrated, not yet economically feasible
- Design for Demise (D4D): proactive solution, gradual adoption

Original Contributions

1. Custom Space Object Detection Model

- deep learning architecture based on CNN, specifically trained for LEO object detection
- custom dataset: 8,596 original images → 13,162 images after augmentation

2. Development of a new component of the MOROI National All-Sky Camera System:

- integration of the solution for Space Situational Awareness (SSA) activities
- automatic frame sorting system for scientific purposes and Space Surveillance and Tracking (SST) monitoring

3. Atmospheric Reentry Analyses of Space Objects

- simulations using the following tools: DAS, DRAMA, and DEBRISK
- assessment of fragment survivability risk for controlled and uncontrolled reentries

Dissemination

DOI

RE-ENTRY SURVIVABILITY ANALYSIS OF ERS-2 SATELLITE

CRISTIAN OMAT[1,2], MIREL BIRLAN[1,4], ALIN NEDELCU[1], VLAD TURCU[3], FLORENT DELEFLIE[4], ULPIA ELENA BOTEZATU[5]

[1]Astronomical Institute of the Romanian Academy, 5 Cuțitul de Argint, Bucharest, 040557, Romania
[2]University of Bucharest, Faculty of Physics, Doctoral School of Physics, 405 Atomistilor street, Magurele, Ilfov, Romania
[3]Cluj-Napoca Astronomical Observatory, 19 Ciresilor, Cluj-Napoca, 400487, Romania
[4]Laboratoire Temps-Espace, Observatoire de Paris, 77 av Denfert-Rochereau, 75014 Paris, France
[5]Romanian Space Agency, 21-25 D. I. Mendeleev street, Bucharest, Romania

Abstract. The history of the ERS-2 satellite is closely linked with that of its predecessor, ERS-1. The first one was launched on July 17, 1991, followed by ERS-2 on April 21, 1995. Both satellites significantly exceeded their original design life of three years, contributing extensively to various scientific and environmental applications during their operational periods. This study focuses on the ERS-2 satellite, whose mission officially ended on September 5, 2011. The final image from ERS-2 was received on July 4, 2011. Subsequently, after executing 66 deorbiting maneuvers, the satellite's altitude was reduced from 780 km to 573 km to facilitate natural orbital decay due to atmospheric drag. Approximately thirteen years later, on February 21, 2024, ERS-2 completed its atmospheric re-entry over the North Pacific Ocean, between Alaska and Hawaii, at the estimated coordinates 37°24'00.0" and 151°54'00.0"W, at 18:17 CET (17:17 UTC).

The objective of this paper is to evalu... of Earth impact by surviving fragments and to estimate the cas... debris. Our analysis assumes that all satellite systems were ...ected, fuel purged, and the wind scatterometer fol... itional data published by ESA in *Bulletin83* ... te model to perform re-entry simulat... ment Software (DAS) develop... NASA), Debris Risk ... ean Space Agency ... es (CNES).

Astronomy and Computing 55 (2026) 101081

Contents lists available at ScienceDirect

Astronomy and Computing

journal homepage: www.elsevier.com/locate/ascom

ELSEVIER

Full length article

Deep learning approach for automated detection of space objects in astronomical imaging

Cristian Omat [a,b,*], Mirel Birlan [a,c], Dan Alin Nedelcu [a], Simon Anghel [c,a]

[a] Astronomical Institute of the Romanian Academy, 5 Cuțitul de Argint, Bucharest, 040557, Romania
[b] University of Bucharest, Faculty of Physics, Doctoral School of Physics, 405 Atomistilor street, Magurele, 077125, Ilfov, Romania
[c] LTE, Observatoire de Paris, Université PSL, Sorbonne Université, Université de Lille, LNE, CNRS, 61 Avenue de l'Observatoire, Paris, 75014, France

ARTICLE INFO

Keywords:
Deep learning
All-sky images
Machine learning
Satellite trail
YOLO
Image processing & techniques

ABSTRACT

The exponential growth in low Earth orbit (LEO) satellite deployments over recent years has introduced substantial challenges for ground-based astronomical observations. Astronomers now routinely encounter satellite trails and space debris crossing their telescope fields of view, necessitating time-intensive manual inspection to identify usable frames for scientific analysis. Simultaneously, detecting and cataloging these objects is essential for building and maintaining Resident Space Object (RSO) catalogs, which support safe and sustainable space operations. This work develops and evaluates a deep learning approach leveraging YOLOv12 to automatically detect satellite and debris trails in all-sky astronomical images. We build a labeled dataset of 7794 FITS images, derived from 8596 raw observations colle... between January 24 and March 23, 2025 and expand it through augmentat... validation, and testing. Our trained models achieve high detection perfor... remaining computationally efficient for real-time use. The trained models ... across different observational conditions, providing an efficient tool for ... quality and supporting Space Situational Awareness through the discovery ... monitoring of cataloged satellites within all-sky monitoring networks.

1. Introduction

All-sky cameras have become a familiar component of small and mid-scale observatories. They are routinely used for night-sky monitoring, cloud coverage assessment, meteor/bolide detection, and public outreach. As a result, there is already a geographically distributed network of inexpensive, continuously operating, wide-field imagers producing long-exposure frames throughout the night. These systems were not originally built for satellite tracking, but they record exactly the kind of evidence, bright linear trails from artificial satellites in low-Earth orbit (LEO) and from larger debris fragments, that is becoming increasingly valuable for Space Surveillance and Tracking (SST).

This is not an abstract concern. The number of active objects and ...

developed, including morphological m... 2016) and neural-network-based syster... 2024), these solutions are often design... telescopes or require significant comput... impractical for small all-sky camera ne... constraints. For many semi-professiona... distributed all-sky camera networks, fr... manually or relies on ad-hoc solutions... increasing satellite density and is prone... data rate from distributed camera array...

Space Surveillance and Tracking (... tary operational modes: survey observ...

DOI

ANALYSIS OF THE RE-ENTRY PHASE OF STARLINK-1353 SATELLITE

CRISTIAN OMAT[1,2], MADALINA TRELIA[1,2], MIREL BIRLAN[1,3], ALIN NEDELCU[1]

[1]Astronomical Institute of the Romanian Academy, 5 Cuțitul de Argint, Bucharest, 040557, Romania
[2]University of Bucharest, Faculty of Physics, Doctoral School of Physics, 405 Atomistilor, Magurele, Ilfov, Romania
[3]Institut de Mécanique Celeste et des Calculs des Ephémérides, CNRS UMR8028, Observatoire de Paris, PSL University, 77 av Denfert-Rochereau, 75014 Paris cedex, France

Abstract. Eighty-three percent of all operational satellites are deplo... Starlink is the largest mega-constellation with 5,233 satellites in... available for June 2024) (Planet4589, 2023). To date, SpaceX ... 6,505 Starlink satellites out of 11,908 units planned (with a... 22,488 units). One of the failed satellites was the Starlink-1... which the controlled decay above Hokkaido Island, on Fe... field-of-view of one telescope from Kitasubaru Astronom... that moment the telescope was performing observatio... in a live streaming session (Kitasubaru, 2024). The ... the video camera of the telescope and based on th... we identified 15 fragments resulted after the atm... analysis based on Debris Assessment Software ... 64.4 km above the sea level and some fragmen... m. The paper presents hypothesis about the ... the sky above Japan and if these can reach ... cal behaviour of Starlink-1353, before th... observation recorded by Berthelot Obs...

1. INTRO...

...ears, the number of op... ...led, the biggest increase bei... ...ions satellites are deployed. ... ...y 100,000 satellites will be active un... organized in some mega-constellations o... ...ms *et al.*, 2021). This unprecedented increase ... low Earth orbits brings many benefits for worldw... deploying satellites in low orbits has a significant impac...

Nos. X, p. 1–17, Bucharest, 2024

a. International conferences

5th International Conference on Space Situational Awareness (ICSSA), Tres Cantos - Madrid, Spania, 7 - 9 aprilie 2026

9th European Conference on Space Debris, Bonn, Germania, 1 - 4 aprilie 2025

64th Israel Annual Conference on Aerospace Sciences (IACAS 2025), Haifa, Israel, 20 martie 2025

8th International Conference in Astronomy, Astrophysics, Space and Planetary Sciences, Cluj-Napoca, 2 - 4 iulie 2025

3ème Édition du Symposium de la Recherche Scientifique Francophone en Europe Centrale et Orientale, Cluj-Napoca, 16 - 17 decembrie

6th International Workshop on Key Topics in Orbit Propagation Applied to Space Situational Awareness (KePASSA), Arras, Franța, 12 - 14 iunie 2024

b. National conferences

Conferința Cercetării Științifice în domeniul Matematicii dedicată împlinirii a 160 de ani de la înființarea Academiei Române, Institutul de Matematică ”Simion Stoilow”, Academia Română, București, 30 - 31 martie 2026

Doctoral Dialogues in Physics 2025, Facultatea de Fizică, Universitatea din București, 10 - 11 octombrie 2025

Bucharest University Faculty of Physics 2025 Meeting, Facultatea de Fizică, Universitatea din București, 23 mai 2025

Bucharest University Faculty of Physics 2024 Meeting, Facultatea de Fizică, Universitatea din București, 24 mai 2024

Modern Techniques in Observational Astronomy, comuna General Berthelot, județul Hunedoara, 1-5 iulie 2024.

Bucharest University Faculty of Physics 2023 Meeting, Facultatea de Fizică, Universitatea din București, 26 mai 2023

Future Work and Perspectives

Probabilistic 3D Position Reconstruction of LEO Objects via Dual-Station Triangulation
for Space Situational Awareness (SSA)

3D Error ellipsoid
resulting from the propagation of astrometric uncertainties and a probabilistic model of the object's 3D orbital position

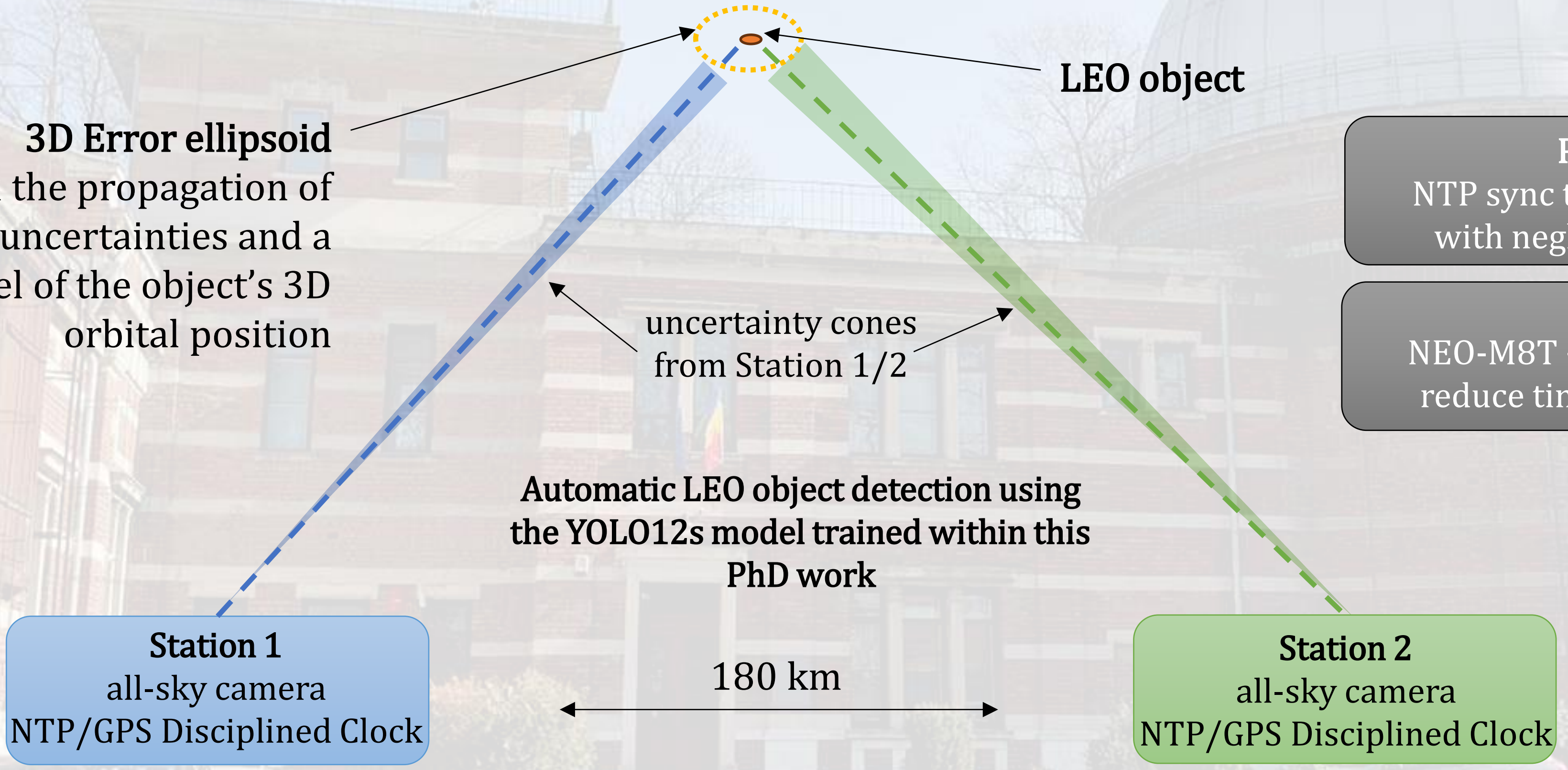

Phase 1: pilot
NTP sync to validate the concept with negligible hardware cost

Phase 2:
NEO-M8T + chrony (Ubuntu) ➔ reduce timing error below 1 μs

Thank you!

I would greatly appreciate your feedback

Please feel free to contact me: **cristian.omat@astro.ro**